Aus dem Institut für Virologie
des Fachbereichs Veterinärmedizin
der Freien Universität Berlin

Mimicking passage of avian Influenza virus through the gastrointestinal tract of chickens and characterization of novel chicken intestinal epithelial cell lines

Inaugural-Dissertation
zur Erlangung des Grades eines
PhD of Biomedical Sciences
an der
Freien Universität Berlin

vorgelegt von
Xuejiao Han
aus Shanxi, Volksrepublik China

Berlin 2020
Journal-Nr.: 4185

Gedruckt mit Genehmigung
des Fachbereichs Veterinärmedizin
der Freien Universität Berlin

Dekan: Univ.-Prof. Dr. Jürgen Zentek
Erster Gutachter: PD Dr. Michael Veit
Zweiter Gutachter: Prof. Dr. Benedikt Kaufer
Dritter Gutachter: Univ.-Prof. Dr. Dr. Hafez Mohamed Hafez

Deskriptoren (nach CAB-Thesaurus): fowls, Influenza viruses, viral hemaglutinins, intestines, inactivation, disease transmission, pH, epithelium, mucosa, Newcastle disease virus

Tag der Promotion: 17.01.2020

Table of contents

List of figures

Abbreviations

aa	Amino acids
CEF	Chicken embryo fibroblast
DMSO	Dimethyl sulfoxide
FP	Fusion peptide
FCS	Fetal calf serum
FPV	Fowl plague virus
GFP	Green fluorescent protein
HA	Hemaglutinin
HAT	Human airway trypsin-like protease
HPAIV	High pathogenic avian Influenza virus
HRP	Horseradish peroxidase
LPAIV	low pathogenic avian Influenza virus
MDCK	Madin-Darby canine kidney cell
NA	Neuraminidase
NDV	Newcastle disease virus
NEP	Nuclear export protein
NP	Nucloprotein
NS1	Non-structural protein 1
PA	Polymerase acidic protein
PB1	Polymerase basic protein 1
PB2	Polymerase basic protein 2
RNP	Ribonucleoprotein complex
TMD	Transmembrane domain
TMPRRS2	Transmembrane protease, serine
vRNA	Viral RNA
vRNP	Viral Ribonucleoprotein complex
WT	Wild type

Amino acids

K	Lys	Lysine
L	Leu	Leucine
R	Arg	Arginine
X	Xaa	any random amino acid

1 Introduction

1.1 Influenza virus

1.1.1 Taxonomy

Influenza virus is a member of the *Orthomyxoviridae* family, which have a segmented negative-stranded RNA genome. Based on the antigenic differences of the nucleoprotein (NP) and the matrixprotein (M1), the virus is divided into type A, B, C and a more recent type D (1,2). Influenza A virus is one of the main public health concerns in both human and veterinary medicine (3,4). Influenza A virus (IAV) is further classified according to the antigenic properties of the two major surface glycoproteins: haemagglutinin (HA) and neuraminidase (NA). Up to date, 18 HA and 11NA subtypes have been identified, among which 16 HA (H1-H16) and 9 NA (N1-N9) subtypes were isolated from bird (5). Aside from birds, various mammalian species were identified as host of IAV as well, such as humans, pigs, bats, horses, cats, mink and marine mammals (1,6). Influenza B viruses could be isolated from humans and seals, whereas Influenza C viruses infect mainly human and swine (7-9). Since 2011, a new Influenza subtype, named Influenza D virus, was isolated from swine and is widely spread in pigs and cattle (2).

1.1.2 Viral genome and proteins

Influenza virus particles have a pleomorphic shape from filamentous to spherical (10). The particles of Influenza A and B are covered by a lipid bilayer envelope in which the virus-encoded glycoproteins hemagglutinin (HA) and neuraminidase (NA) and a proton channel (called M2) are embedded (11). By contrast, in Influenza C and D virus, the only spike protein, hemagglutinin-esterase-fusion (HEF) protein combines the functions of both HA and NA (12). Beneath the envelope is a shell composed of the matrix protein (M1) and in the interior of the virus are the viral genome segments and a protein called nuclear export protein (NEP). The Influenza viruses have a segmented single-stranded RNA genome: Influenza A and B viruses contain eight distinct segments, and Influenza C and D viruses contain seven segments, each encodes one or more viral protein(s). Viral RNA (vRNA) of each segment is bound to the polymerase complex and to multiple copies of nucleoprotein (NP), which together form the viral ribonucleoprotein (vRNP) complexes. The heterotrimeric viral RNA-dependent RNA polymerase (RdRp) is composed of three subunits: polymerase basic 1 (PB1), polymerase basic 2 (PB2) and polymerase acidic (PA) in Influenza A and B or polymerase 3 (P3) in Influenza C (11,12).

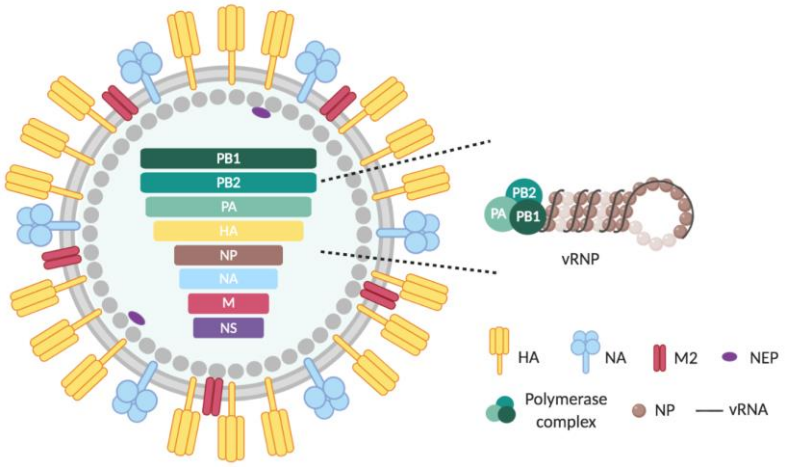

Fig.1.1 Scheme of a typical spherical Influenza A virus.

The spike proteins hemagglutinin (HA), neuraminidase (NA) and the ion channel M2 are inserted into the outer lipid membrane of the virus. The matrix protein M1 underlies the lipid layer. The interior of the virus contains the segmented genome, viral ribonucleoproteins (vRNPs), each of which encodes one or more proteins. The RNPs are composed of the polymerase complex [consisting of polymerase basic protein 1 (PB1), protein 2 (PB2) and polymerase acidic protein (PA)], multiple copies of nucleoprotein (NP) and viral RNA (vRNA) that is wrapping the NP. The interior of the virion also contains a minor protein called nuclear export protein (NEP).

1.1.3 Pathogenesis, tissue distribution and transmission of Avian Influenza viruses (AIV)

Wild aquatic fowls in the order of Anseriformes (particularly ducks, geese, and swans) and Charadriiformes (particularly gulls, terns, and shorebirds) are the natural reservoirs of AIV. In most cases, AIV cause infections in wild birds without obvious signs of disease. These wild waterfowls potentially distribute viruses to domestic birds during migration. AIV infection of domestic birds may cause a wide range of clinical syndromes ranging from subclinical infection, mild to severe disease and death (13,14). According to the OIE manual, AIV that can cause a mortality of over 75% within 10 days are classified as highly pathogenic, while others that do not reach this standard are classified as low pathogenic (15). The term “highly pathogenic” or “low pathogenic” does not indicate the exact same viral pathogenesis in other bird species. The pathogenesis is a complicated feature determined by the viral strain, host adaptation and factors, such as environment and secondary bacterial infections (16).

AIV pathogenesis and tissue distribution were mainly studied in a few species, mainly in ducks, chickens and turkeys. In gallinaceous poultry like chickens and turkeys, HPAIV first infect the epithelium of the upper respiratory tract, then the submucosal capillary endothelium and spread widely over multiple organs (14,17). The infection spread so rapidly that chickens and turkeys may not present apparent clinical signs before their sudden death and the mortality can reach up to 100% (18). Birds in peracute and acute stage could be depressed, exhibit ataxia or even become lethargic with reduced consumption of food and water. Birds that survive this acute stage might show neurological and respiratory signs. After dissection, gross lesions can be seen in multiple visceral organs, the cardiovascular and nervous systems and the skin. In general, haemorrhage appears in skin, lung, digestive tract (especially the mucosa of the proventriculus and ventriculus), epicardium and coronary fat of heart and skeletal muscles. Pale foci of necrosis may be present in the heart and visceral organs like the pancreas and spleen (17-21). Most HPAIV do not cause clinical signs or lesions in non-gallinaceous birds like ducks, with the exception of some lineages of Eurasian H5H1 strain. These H5N1 linages infect domestic ducks and caused damage in the respiratory tract, the pancreas, central nervous system, adrenal glands, and myocardium in an age-dependent manner. Overall, HPAIV infect multiple organs, spread systemically and are shed from the respiratory and intestinal tracts (14,22-25).

LPAIV initially infect nasal epithelium cells and then replicate in respiratory and digestive tract of gallinaceous birds. LPAIV infection may be subclinical or result in clinical disease with high morbidity but low mortality (20). Gross lesions can be seen in the upper respiratory tract (rhinitis, sinusitis, laryngitis, and tracheitis). Egg-production chickens may show lesions in their reproductive system and misshaped, or pigment-loss eggs could be produced. Turkeys are more susceptible than chickens with lesions like enteritis and pancreatic damages (16,19,21).

For non-gallinaceous birds, LPAIV replication initiates in enterocytes (in mallards) or the bursa of Fabricius (in young duck) and virus shed in the feces reaches a concentration of 10^7 EDIT50/g. Clinical signs are rarely observed or non-specific in these species (26-28). Co-infection or secondary infection of bacterial pathogen might result in higher mortality rate (16,19). Transmission of LPAIV between birds is believed to occur primarily via the faecal-oral route, although other routes are possible (29).

1.1.4 Reverse genetics of Influenza viruses

In the opposite direction of forward genetics, reverse genetics serves as an approach to reveal the function of a gene by making mutations followed by detecting and analyzing their phenotypic effects. Reverse genetic system in RNA viruses requires the de novo generation of virus from a cDNA clone. Unlike positive-strand RNA viruses, viral RNAs (vRNAs) of negative-strand RNA viruses cannot be directly used as a template for viral mRNA and protein synthesis. Thus, the viral ribonucleoprotein (vRNP) complex composed of vRNA, polymerase complex and nucleoprotein is needed (30).

The early reverse-genetics systems for Influenza A virus were developed with the presence of a helper Influenza virus. In the first method, vRNAs were synthesized in vitro and reconstituted with purified viral proteins, then vRNPs were transfected into cells. In the second method, Influenza cDNAs were cloned and inserted between polymerase I promoter and terminator sequences in a plasmid. vRNPs were produced in vivo after transfection of vRNA encoding plasmids (31,32). Both methods rely on infection with helper virus, thus a selection system is required to distinguish the desired virus from helper virus background (33).

In 1999, a purely plasmid based reverse genetic system was established. In this system, cDNA of eight vRNA segments were cloned and inserted between the human RNA polymerase I promoter and the mouse RNA polymerase I terminator in the plasmid pHH21 to form vRNA expressing plasmids. At the same time, cDNAs of four viral polymerase complex proteins were cloned into the chicken actin promoter controlled eukaryotic expression vector pCAGGS-MCS. All 12 plasmids were cotransfected into human embryonic kidney cells (293T), resulting a high viral yield (34). The very next year, the system was updated, while the entire RNA polymerase I transcription unit was flanked by an RNA polymerase II (pol II) promoter and a polyadenylation site. This pol I–pol II system transcribe negative-sense vRNAs with pol I promotor and positive-sense mRNAs (which will be translated into viral proteins) with pol II promotor from one set of viral cDNA template but with an opposite transcription direction, resulting a reduction in the number of plasmids required for Influenza A virus rescue (35). With the same principle and technology, generation of Influenza B and C viruses with only plasmids were achieved (36,37).

Other groups constructed a multi-unit plasmid that contains all the required constituents, and with the help of dual promoters, successfully generate Influenza virus. Also, reverse genetic systems recruiting chicken, canine and mouse RNApolI promoters were established to overcome the limitation of promotor species specificity of former systems and allow rescue of virus from CEF, MDCK and BHK cells, respectively (38-40).

Plasmid-based reverse genetics techniques have allowed researchers to generate wild type and mutant viruses from full-length cDNA copies of the Influenza viral genome. By genetically engineering infectious recombinant viruses through site-directed mutagenesis, gene insertion or deletion, functions of specific viral genome can be determined, which allow a better understanding of viral pathogenesis, transmissibility, and host-range interactions (33,41).

Furthermore, recombined virus particle production by reverse genetics also facilitate the development of alternative vaccines (42).

1.1.5 Cells used for Influenza study

Embryonated chicken eggs are universally used for virus isolation and propagation. Viruses were inoculated into the allantoic cavity of 10-day-old embryonated eggs with needle and syringe. Influenza viruses replicate in cells of chorioallantoic membrane and high titers of virus can be recovered from the allantoic fluid 2-3 days after inoculation (43).

The most common cellular model for Influenza virus studies is the Madin–Darby canine kidney (MDCK) cell, which was first described by Mardin and Darby (44). MDCK cells are easy to handle, they grow in a wide pH range, are easily recovered by thawing after liquid nitrogen storage, and are not too sensitive to centrifugation. Moreover, they are susceptible to various Influenza strains, and thus are wildly used for primary isolation of Influenza, virus propagation and plaque assay since 1960s (45,47). Later, mechanism of virus entry, the biology function of viral proteins and anti-viral activities of cellular inhibitors were studied in MDCK cells (48-50). Since they exhibit an epithelial phenotype, polarized MDCK cells were used as epithelial model to investigate intracellular sorting and transport of viral components (51,52). MDCK cells of different origins and passages were used in different laboratories (53). MDCK derivatives were generated for special purposes. For example, MDCK-SIAT1 are modified to express increased level of α-2,6 lineage sialyltransferase, and are reported to exhibit an improved isolation of human Influenza virus from clinical specimens and viruses displayed higher gene stability in it (54). Furthermore, development of large scale cell culture technology made it possible to produce cell-based Influenza vaccines. For example, Optaflu/Flucelvax, a trivalent subunit human Influenza vaccine, was produced in MDCK 33016 cells adapted to grow in suspension in a serum and protein-free medium (55).

African green monkey kidney epithelial cell (Vero) also serves as a suitable system for primary isolation and cultivation of Influenza A and B viruses (56). It differs from MDCK cells in interferon production and glycosylation after Influenza infection, but produce virus particles equally well as MDCK cells (57). Vero cells were further used for protein function studies and vaccine production (58). Trivalent and monovalent vaccines were produced in Vero cells and licensed (59). Besides, baby hamster kidney (BHK) cells and human lung carcinoma cell line A549, which are derived from mammalian tissues, also facilitate Influenza research (60,61).

In recent decades, epithelial cells from different origins were established and used as cellular models for analysis of virus-host interactions, as listed in Table 1.1. Primary cell culture from native target tissues, such as swine respiratory tract, chicken kidney and intestine, as well as duck endothelium, ferret nasal epithelium, minimize the genetic variations and serve as an excellent cell system to study the host susceptibility (62-66). Immortalized epithelial cell lines from the respiratory tract of human, mouse, pig, chicken and dog, as well as porcine intestinal tract, were used to overcome the setback of primary cells, while they remain constant after passaging for numerous generations (67-74). In this year, human monocytic cell U937 was established and used especially in cytokine production studies (75).

In the field of Influenza vaccine production, cell-based production technology shows advantages over traditional egg-based production processes, for example, shorter production cycles, faster respond to market needs, better process control and less allergic reactions (76). Beside MDCK and Vero cell, manufacturers are interested in designer cell lines that are derived

from human or animal cells. Possible candidates include human cell lines PER.C6 cells (human retinoblast), HEK293 cells, CAP cells (human amniocytes) and avian cell lines duck EB14/ EB66 cells (derived from duck embryonic stem cells), duck AGE.CR and AGE.CR.pIX cells (derived from duck retinal cells), duck DuckCelt-T17 cell (duck embryo cell) and quail QOR/2E11 cells. The production processes are still under development focusing on cell scaling condition and optimization of the Influenza virus propagation process (77-80).

1.2 Hemagglutinin of Influenza A virus

1.2.1 Hemagglutinin synthesis and structure

Hemagglutinin (HA) is the major glycoprotein of Influenza virus. It is inserted into the viral envelope as a type I transmembrane protein. 18 different HA subtypes were determined by nucleotide sequences. The precursor HA0 has a size of about 75kD, is synthesized at the rough endoplasmic reticulum (rER) and then transported via the ER and the Golgi network to the plasma membrane, and finally assembles with other viral proteins. Along the secretory pathway, HA0 is folded, forms a homotrimer, and is N-glycosylated and palmitoylated (81, 82). The precursor HA0 protein needs to be cleaved proteolytically by proteases into HA1 (ca. 50kD) and HA2 (ca. 25kD) subunits to exert its function. The cleavage occurs at a conserved arginine-glycine bond located in a loop that protrudes from the surface of the membrane-proximal third of the HA molecule. Cleavage can happen at different stages during HA maturation, either in the host cell or extracellularly after progeny virus release. The HA1 subunit contains the receptor binding site, and the HA2 subunit is membrane anchored and responsible for fusion. The crystal structure of trimeric HA shows a globular head domain, which consists exclusively of HA1, and a stalk domain composed of HA2 and the C-terminal part of the HA1 subunit (82).

1.2.2 HA cleavage

1.2.2.1 HA cleavage determines the pathogenicity of avian Influenza viruses

The variations in the amino acid sequence and the conformation of the loop determines by which proteases HA is cleaved. In avian Influenza viruses, the amino acid sequence in the loop determines the pathogenicity. Highly pathogenic avian Influenza viruses (HPAIV) have the multibasic consensus motif R-X-R/K-R (arginine R, lysine K), which can be recognized and cleaved by an ubiquitous protease. Thus, HAs with multibasic amino acids are proteolytic cleaved in multiple organs and tissues, causing systemic infection and fatal disease in birds. HPAIV occurs only within subtypes H5 and H7 in nature, but not all H5 and H7 strains are highly pathogenic since most lack a polybasic cleavage site (81, 83).

In contrast to HPAIV, low pathogenic avian Influenza virus (LPAIV) and mammalian Influenza strains have a single R (or rarely a single K in AIV) at the monobasic cleavage site that are cleaved by trypsin in vitro. Trypsin-like proteases are expressed only in the respiratory and the intestinal tract of birds and in the respiratory tract of mammal, thus confining the spread of the viruses to these organs. LPAIV cause mild or asymptomatic infections in the intestinal and the respiratory tract of birds and spread via the oral-fecal route (81, 83, 84).

Table 1.1 Established cells used for Influenza study

Cells	characters	Ref.
Human and mouse airway epithelium cell (hTEC and mTEC)	• 2,3-linked SA receptor was expressed in both cells. • 2,6-linked SA receptor was not expressed in the mTEC	(67)
Human nasal epithelial cell (hNEC)	• seasonal H1N1 Influenza virus replicated to higher titers than live attenuated Influenza vaccine (LAIV) strain in hNEC cultures • the supernatants from H1N1 and LAIV strain infected hNEC cultures showed equivalent amounts of viral proteins and HA titers, suggesting the formation of non-infectious virus particles when hNEC infected with LAIV	(68)
Porcine lung epithelial cell line (SJPL)	• 14 mammalian- and 15 avian-Influenza A strains, as well as 1 Influenza B strain replicated in this cell line, with a comparable to or better infectivity titers of most viruses in SJPL cells than those in MDCK cells. • The numbers of both 2,3-linked SA and 2,6-linked SA receptors on SJPL cells were greater than those on MDCK cells	(69)
Porcine intestinal epithelial cell line (SD-PJEC)	• preferentially expresses 2,6-linked SA receptor • permissive to human and swine Influenza A viruses and some avian Influenza viruses, but poorly support the growth of Influenza B viruses • able to rescue swine-origin Influenza viruses in conjunction with 293T cells	(70)
Porcine primary respiratory epithelial cells	• higher expression levels of 2,6-linked SA than 2,3-linked SA receptors • supported the replication of Influenza A, B, C, and D viruses in virus type and temperature dependent manner	(62)

Porcine bronchial epithelial cells (hTERT-PBECs)	• were susceptible to swine Influenza virus of H3N2 subtype	(71)
Porcine airway epithelial cells (MK1-OSU)	• express both 2,6-linked SA and 2,3-linked SA receptors • susceptible to swine Influenza A, but not to human B and C viruses. Also permissive to infection by Influenza D virus	(72)
Chicken lung epithelial cell (CLEC213)	• support efficient growth of the LPAIV H6N2 in the presence or the absence of trypsin • able to mount a robust cytokine and chemokine immune response to viral infection	(73)
Chicken primary intestinal epithelial cell	• highly susceptible to LPAIV H9N2 and NDV Herts 33/56 • IFN λ increased more than 30 fold when infected with H9N2	(64)
Duck primary endothelial cell	• susceptible to an H5N1 HPAI virus but to a much lesser extent than chicken endothelial cells	(65)
Canine tracheal epithelial cell line (KU-CBE)	• express 2,3-linked SA, but not 2,6-linked SA • susceptible to canine Influenza virus	(74)
Ferret primary nasal epithelial cell (FNEC)	• both 2,6-linked and 2,3-linked sialic acid (SA) receptors were detected on the apical surface of the culture • a pre-2009 seasonal A(H1N1) virus infected both ciliated and nonciliated cells, whereas a highly pathogenic avian Influenza (HPAI) A(H5N1) virus primarily infected nonciliated cells	(66)
human monocytic cell U937	• support the replication of H1N1, H3N2, H7N8 Influenza A viruses and an Influenza B strain • produce important pro-inflammatory cytokines	(75)

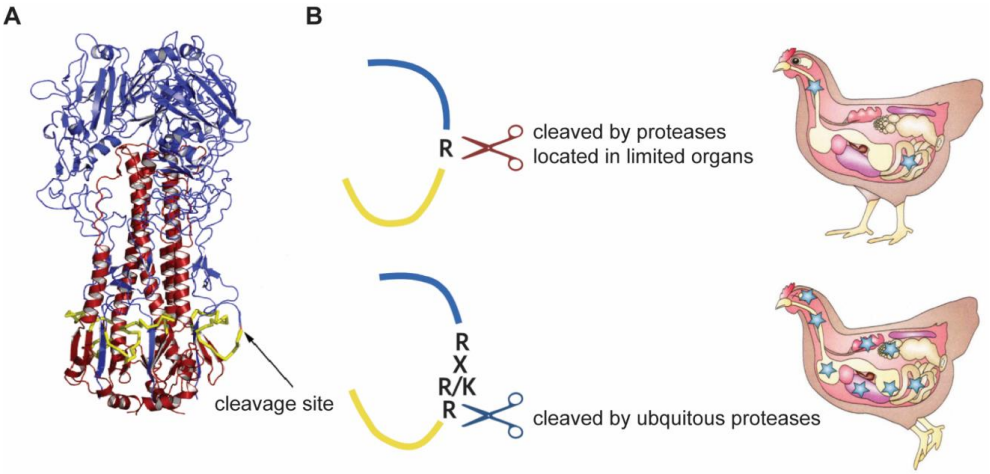

Fig.1.2 HA cleavage and protease determined pathogenicity of AIV.

(A) The precursor HA0 is proteolytic cleaved into HA1 and HA2 subunits at a loop projecting from the surface of the molecule. This figure is reprinted from with permission. **(B)** HA0 with a single R at the cleavage site can be cleaved by trypsin-like proteases, which are expressed only in the respiratory and the intestinal tract of birds, thus restricting the virus replication to these sites and cause (sub)clinical disease. Viruses with these HA0 are low pathogenic avian Influenza viruses (LPAIV). Some viruses from H5 or H7 subtype contain a multibasic consensus motif R-X-R/K-R in the HA cleavage site which can be cleaved by ubiquitous proteases. Thus, such viruses spread systemically in the body of infected birds and induce lethal diseases and cause high mortality, which are defined as high pathogenic avian Influenza viruses (HPAIV).

1.2.2.2 Proteases that activate HPAIV and their inhibitors

HA with several basic amino acids in the cleavage site is cleaved by the ubiquitous endoproteases furin. Furin belongs to the family of eukaryotic subtilisin-like serine endoproteases and also cleaves the fusion proteins of other enveloped viruses (e.g., HIV, dengue fever virus and several filoviruses) as well as bacterial toxins (e.g., anthrax toxin, botulinum toxin). Furin is located mainly in the trans-Golgi network (TGN) and is transported to the plasma membrane via the constitutive secretory pathway and partially retrieved back to the TGN through the endosomal system. Furin co-localize with HA in the TGN and that is where cleavage occurs (85). The proprotein convertase 5/6 (PC5/6), which shares similarities with furin in structure and substrate specificity, also activates HAs with multibasic cleavage site, whereas other members of proprotein convertases, i.e. PC1/3, PC2, PC4, PACE4, PC7, SKI-1/S1P, and PCSK9, do not cleave multibasic HAs (86).

Several inhibitors of furin have been developed. Optimized inhibitors show significant inhibitory activity and stability under physiological conditions and thus are tested as potential antiviral drugs. For example, the furin inhibitor MI-701 was tested in animal experiments, either applied alone or in combination with conventional antiviral compounds. Replication of the HPAIV strains A/Thailand/1(KAN-1)/2004 (H5N1) and A/FPV/Rostock/1934 (H7N1) in chicken were reduced after treatment with MI-701 alone in a concentration-dependent manner. The inhibitory efficacy is further enhanced by combined treatment of MI-701 with oseltamivir or favipiravir and triple combination with oseltamivir and ribavirin (87).

1.2.2.3 Host cell proteases identified to cleave HA with monobasic cleavage site

1.2.2.3.1 Identified host cell proteases

HA of LPAIV is cleaved in embryonated chicken eggs by a blood clotting factor Xa like protein, and other trypsin-like proteases, such as plasmin and tryptase Clara, have been identified to activate HA with a monobasic cleavage site in vitro (88). Many host cell proteases that can activate monobasic HAs in the human airway epithelium cells were identified as shown in Table 1.2.

In 2006, the transmembrane protease serine 2 (TMPRSS2) and HAT (human airway trypsin-like protease, also called TMPRSS11d) from human airway epithelium cells were first identified as cellular HA-activating proteases (89, 90). TMPRSS2 and HAT belongs to type II transmembrane serine proteases (TTSPs) family, which is a group of cell surface-associated proteases playing important roles in the development and homeostasis of mammalian tissues. Expression of either protease enables H1, H2, H3 LPAI strains to multiply in MDCK cells without exogenous trypsin (91). Cleavage of 16 HA subtypes was tested in cell by coexpression of HA0 with either TMPRSS2 or HAT. The results showed that cleavage by TMPRSS2 was more efficient than that by HAT, while H12 HA was the only HA examined showing greater cleavage by HAT (92). TMPRSS2-knockout mice did not show any signs of disease or body weight loss compare to wild type mice when infected with H1N1 and H7N9 strains; results from HAT-knockout in vivo experiments are still missing (93-95).

Another member from TTSPs identified as HA-activating protease is TMPRSS4. Knockdown of TMPRSS4 reduced H1N1 virus replication in human intestinal epithelium Caco-2 cell (96). However, infection of mice with the H3N2 strain was significantly reduced, but not completely inhibited when both TMPRSS2 and TMPRSS4 genes were knocked out, indicating that other proteases can cleave HA of the H3N2 strain (97).

Besides, matiptase, DESC1, MSPL and TMPRSS11A of the same family also showed HA cleavage activity in a HA-subtype and strain specific manner. Results were mainly obtained by in vitro coexpression of HA with a certain protease, further data on the in vivo relevance are still missing (98, 101).

Additionally, kallikrein (KLK) types 5 and 12 were tested for HA activation. HA of HA1 and HA3 were cleaved when cotransfected with KLK5, while KLK12 cleaves HA of H1 and H2 subtype. KLK5 treatment enables the infection of both H1 and H3 viruses in MDCK, but only H3N2 tested strain is promoted to infect mice after KLK5 pretreatment (102, 103).

Studies on HA-activating protease mostly focused on those expressed in human airway epithelium. Similar proteases in the avian respiratory and gastrointestinal tract are not deeply investigated. More recently, chicken ubiquitin-specific protease 18 (chUSP18) was reported to enhance the replication of a recombinant LPAIV, but not an HPAIV, indicating its potential function in LPAIV HA cleavage (105).

Although several proteases that cleave HAs with monobasic motif were identified, a knowledge gap still exist. It is a complex task due to several reasons. Firstly, protease activity shows a clear HA subtype or even strain specificity, which may be related to the structure of the cleavage site loop and adjacent carbohydrate moieties. Secondly, as the result of TMPRSS2/TMPRSS4 knock-out mice indicated, two or more proteases might have the function of HA processing, whether they work synergistically and if other protease will compensate when one or two are knocked out is not clear. Last but not least, coexpressing HA

and protease candidates in cells and detecting HA cleavage or infectivity enhancement are the commonly used method to identify activating proteases. Clear limitations exist while expressed HA might not expose cleavage loop the same way as *in vivo*, cleavage of HA doesn't enhance virus infectivity, and promoted infectivity in cell isn't necessarily relevant to that in vivo.

1.2.2.3.2 Distribution and localization of HA cleaving proteases

TMPRSS2 is widely detected in epithelial cells of human respiratory, gastrointestinal and urogenital tract and HAT is mainly found in the trachea and bronchi as well as in the gastrointestinal tract, the skin and the brain. Homologous proteases exist in swine and mice and share similar characteristics in subcellular localization and substrate specificity with those in human (90, 107).

TTSPs are predicted to be located in the plasma membrane with an extracellular catalytic domain. Soluble HAT and TMPRSS2 are present in cell supernatants, however they don't activate virus particles with uncleaved HA0. In polarized epithelial cells, HAT mainly accumulate on basolateral and apical surfaces while TMPRSS2 is distributed at intracellular membranes and at the apical surface. Subcellular localization of proteases strongly suggests that TMPRSS2 cleaves newly synthesized HA0 in the TGN, while HAT activates both released and incoming virions at the plasma membrane (90).

1.2.2.3.3 Airway proteases inhibitors as potential antiviral strategy

Considering their importance in Influenza activating and spreading, airway proteases are obviously potential drug targets. The first synthetic inhibitors of TMPRSS2 were identified by expressing the catalytic domain and screening with various trypsin-like serine protease inhibitors. MI-432, which is derived from sulfonylated 3- amindinophenylalanylamide derivatives, was considered to be the most potent analogue with a Ki value of 0.9 nM as well as its ability to block H1N1 and H3N2 growth in human airway epithelial cells. Similarly, synthesized inhibitors of HAT and matriptase were identified to display low Ki values and virus blockage ability (108). Taken together, optimized synthetic protease inhibitors are expected to become efficient antiviral drug, especially in combination with other antiviral agents.

Table 1.2 Identified cellular proteases that cleave monobasic HA

Protease	HA origin	Evidence of HA cleavage	Ref.
TMPRSS2	A/Memphis/14/96 (H1N1) A/Mallard/Alberta/205/98 (H2N9) A/Texas/6/96 (H3N2) A/turkey/Wisconsin/1/66 (H9N2) A/quail/Shantou/782/00 (H9N2) A/quail/Shantou/2061/00(H9N2)	expression of TMPRSS2 in MDCK cells enabled multicycle replication of viruses in the absence of exogenous trypsin	(91, 100)
	A/Puerto Rico/8/34 (H1N1)	HA is cleaved in TMPRSS2- expressing Caco-2 cell. Knockdown of TMPRSS2 reduces H1N1 virus replication in Caco-2.	(96)
	A/Puerto Rico/8/34 (H1N1) A/Hamburg/4/2009 (H1N1) A/Anhui/1/13 (H7N9) A/California/04/09 (H1N1)	TMPRSS2-knock-out mice did not exhibit body weight loss and showed no signs of disease when infected	(93, 95)
HAT(TMPRSS11d)	A/Memphis/14/96 (H1N1) A/Mallard/Alberta/205/98 (H2N9) A/Texas/6/96 (H3N2)	expression of HAT in MDCK cells enabled multicycle replication of viruses in the absence of exogenous trypsin	(91)
TMPRSS4	A/Puerto Rico/8/34 (H1N1)	HA is cleaved in TMPRSS4- expressing cell. Knockdown of TMPRSS4 reduces H1N1 virus replication in Caco-2.	(96)
	A/Hong Kong/01/68 (H3N2)	TMPRSS2/TMPRSS4 double-knockout mice showed a remarkably reduced body weight loss, mortality, virus spread and lung pathology	(97)
matriptase	A/Puerto Rico/8/34 (H1N1) A/New Caledonia/20/99 (H1N1) A/California/04/09 (H1N1)	HA is cleaved when it's cotransfected with matriptase in a subtype and strain specific manner.	(98)

	A/quail/Shantou/782/00 (H9N2) A/quail/Shantou/2061/00 (H9N2)	Matriptase expressing MDCK and CEK cells enabled multicycle replication of viruses in the absence of exogenous trypsin	(99)
	A/Puerto Rico/8/34 (H1N1)	knockdown of matriptase significantly blocked virus replication in matriptase expressing human bronchial epithelial cells	(100)
DESC1 and MSPL	A/South Carolina/1/1918 (H1N1) A/Singapore/1/57 (H2N2) A/Hong Kong/1/1968 (H3N2) A/Puerto Rico/8/34 (H1N1) A/Panama/2007/1999 (H3N2)	Transfected HA1, HA2 and HA3 were cleaved in DESC1 or MSPL expressing cell. DESC1 and MSPL expressing 293T cells enabled HA cleavage after infection	(101)
KLK5	A/California/04/09 (H1N1) A/WSN/33 (H1N1) A/Aichi/2/68 (H3N2) A/Wyoming/3/03 (H3N2) A/Wisconsin/67/05 (H3N2)	HA is cleaved when cotransfected with KLK5 in mammalian cells.	(102)
	A/Puerto Rico/8/34 (H1N1) A/Scotland/20/74 (H3N2)	KLK5 promotes the infectivity of both virus in MDCK, but only A/Scotland/20/74 is infectious to mice after treatment with KLK5.	(103)
KLK12	A/Puerto Rico/8/34 (H1N1) A/California/09(H1N1) A/Japan/305/57(H2N2)	HA is cleaved when cotransfected with KLK12 in mammalian cells.	(102)
TMPRSS11A	A/Puerto Rico/8/34 (H1N1) A/Panama/2007/1999 (H3N2)	TMPRSS11A expressing 293T cells enabled HA cleavage after infection. But cleavage was not blocked by HAI-1	(104)
chUSP18	A/chicken/Yokohama/aq55/2001	chUSP18–overexpressing DF-1 cells enhance virus growth	(105)
hepsin	1918 Influenza virus	Cleave HA when hepsin-expressing plasmid co-trransfect with HA-expressing plasimid, but do not activate Influenza virus	(106)

1.2.3 Roles of HA in viral entry

1.2.3.1 Receptor binding site and its specificity

One major function of HA protein is binding to cellular receptors. The receptor binding site (RBS) is at the top of the HA1 molecule, and is composed of a short 190 helix at the membrane distal edge, a 130 loop region at the proximal boundary, a 150 loop at the right side, a 220 loop at the left side, and a base part composed of conserved residues in all subtypes of Influenza, which include Tyr98, Trp153, His183, and Tyr195 (109).

HA of Influenza A and B viruses binds multivalently to non-O-acetylated N-acetylneuraminic acid (Neu5Ac), a member of the sialic acid family. In vivo, the sialic acid moieties expose in terminal of glycoproteins and glycolipids on the surface of cells (110). The receptor binding property of the viral HA is a basic determinant of its host range: HA from human viruses preferentially recognize α2-6 linked sialic acid, those from avian and equine viruses have a higher affinity to α2-3 linked sialic acid, and HA from swine viruses can recognize both types. Furthermore, the fine receptor specificity is not identical among different avian strains. For example, duck viruses prefer the β1-3 bond between the terminal Neu5Ac 2-3Gal moiety and the next sugar residue, while other stains from gull or chickens prefer the β1-4 bond (83, 110).

Changing of certain residue in RBS could alter the preference of receptor type and thus adapt the virus to different host. For example, avian H1N1 virus obtained the mutations E190D and G225D in its conserved RBS of HA after transmission to humans. The virus with the single mutation E190D acquired the ability to bind to α2-6 linked receptors, which is associated with a decrease in its affinity for α2-3 linked receptors; a double mutant (E190D, G225D) mainly bound to α2-6 linked receptors (111, 112). Thus, viruses containing these mutations successfully transmitted among humans resulting in a pandemic in 1918 and so did other pandemic strains in history. Other critical amino acid changes or glycosylation of HA in host cell might also alter its receptor specificity (110).

On the other hand, differences in the presence of receptors on the cell surface at least partially determine the susceptibility to Influenza virus infection. Using Sia-binding lectins, Maackia amurensis agglutinin (MAA), which binds to Neu5Ac 2-3Gal moieties and Sambucus nigra agglutinin (SNA), which recognizes Neu5Ac 2-6Gal, the receptor distribution in native host tissues and cells were determined. Cells in the human upper respiratory tract (nasal, tracheal and bronchial epithelium) are abundant in α2,6-linked glycans, while the lower respiratory tract (terminal bronchioles, alveoli) contains both α2,3- and α2,6-linked glycans (113, 114). Swine (115, 116) shows a similar sialic acid linkage-type distribution as humans. Cultured primary swine trachea epithelial cells (117), as well as ex vivo swine tracheal and lung tissues (118) showed a complex distribution of both glycans, with a greater abundance of α2,6 glycans. By contrast, non-human primates and mice express more α2,3 sialic acid. There is a greater variation in receptor distribution among avian species depending on species and examined tissues. For instance, duck intestine exclusively displayed α2,3-linked receptors, while α-2,3 and α-2,6 receptors were present in the respiratory and intestinal tracts of the chicken, turkey and other birds (119, 120). The sialic acid distributions also agrees with the fact that avian hosts transmit viruses via the fecal-oral route, while humans and pigs transmit viruses mainly through respiratory droplets.

1.2.3.2 Membrane fusion and HA stability

Receptor-bound virus enter the cell by endocytosis and then viral particles are transported to endosomes (82). Fusion of the viral membrane with the endosomal membrane starts when HA is activated by the acidic pH of endosomes and is accomplished through a series of steps. First, slightly acidic pH in the endosomes induces an irreversible conformational change of the HA2 subunit which exposes its N-terminal fusion peptide. The hydrophobic fusion peptide inserts like an anchor into the endosomal membrane and interacts with lipid acyl chains. Several HA molecules form a cluster, called the fusogenic unit. The HA fusogenic unit then undergoes a further conformational change, pulling the outer leaflets of the opposing membranes together and inducing lipid curvatures to form a hemifusion stalk. Later, the stalk collapses to form a fusion pore through which the viral genetic material is eventually transferred into the cytosol (110).

The pH of fusion, i.e. the pH value at which the irreversible conformational changes are induced, is different in HA of different Influenza strains (within a range of pH 4.8–6.2) and is considered to be another parameter that plays a role in virus host-specificity and pathogenicity (92). Taking H1N1 subtype as an example, HA activating pH values of avian H1N1 strains are between 5.0-5.2, while Eurasian avian-like swine viruses fuse at a pH between 5.1-5.4 (121). Furthermore, the fusion pH decreased during the evolution from precursors in swine (pH 5.5–6.0) to early and later human isolates (pH 5.2–5.5) (122). Such differences could be due to the variation of endosomal pH among different cells that determines the time point of fusion. When exposed to an improper pH, the HA protein could not make the conformational changes that is required to cause membrane fusion in the endosome, and thus is inactivated.

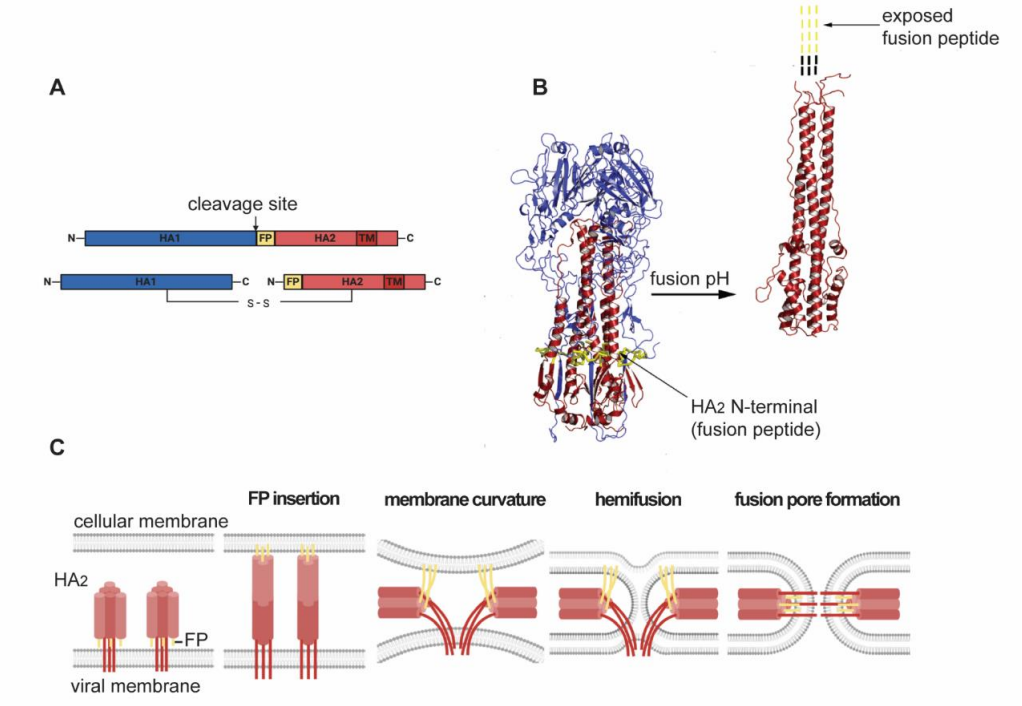

Fig.1.3 HA induced membrane fusion.

(A) The scheme of HA0 cleavage. The fusion peptide is located at the N-terminal of HA2. **(B)** Structural changes in the HA protein after low-pH induced activation. This figure is reprinted from with permission. **(C)** The scheme of HA induced fusion procedure.

1.3 Newcastle disease virus

Newcastle disease (ND) is one of the most widely distributed infectious diseases of poultry. The viral agent is Newcastle disease virus (NDV), a member of the family of *Paramyxoviridae* that is able to infect over 240 species of birds (123, 124).

1.3.1 Viral genome and structure

NDV is an enveloped virus with a non-segmented, negative sense, single stranded RNA genome. The typical NDV genome contains six open reading frames (ORF), which encode the nucleocapsid protein (N), matrix protein (M), phosphoprotein (P), fusion protein (F), haemagglutinin-neuraminidase protein (HN), and large polymerase protein (L). Each of the genes encode one major protein except the P gene that encodes three proteins (P, V and W) (125).

The envelope of the virus is covered by two surface proteins, F and HN, which are responsible for virus attachment to and subsequent fusion with the host cell. The M protein is present beneath the envelope and is responsible for virus assembly and budding. The interior of the virus particle contains the nucleocapsid core composed of the N protein and the genomic RNA to which P and L proteins are bound (126).

1.3.2 Virulence and viral protein

The mean death time (MDT) in embryonated chicken eggs is commonly used as assessment of NDV´s virulence. Lentogenic NDV strains are low virulent, causing subclinical infection with mild respiratory or enteric symptoms and have a MDT of more than 90 hours. Mesogenic NDV strains are intermediate virulent, causing respiratory infection with moderate mortality (< 10%) and have a MDT between 60 to 90 hours. Velogenic NDV strains are of high virulence causing up to 100% of mortality and have a MDT less than 60 hours. Velogenic strains are further classified into viscerotropic velogenic and neurotropic velogenic strains (127). Other methods to assess NDV´s virulence include the intravenous pathogenicity index (IVPI) in six-week-old chickens and the intracerebral pathogenicity index (ICPI) in one-day-old chickens (128).

The surface glycoprotein F, is supposed to be the major determinant of virulence. Similar to the HA protein of Influenza virus, the F protein is synthesized as a precursor F0, which requires proteolytic cleavage into F1 and F2 to fully activate its function to fuse the viral membrane with a host cell membrane. The velogenic and mesogenic strains have the sequence 112R/K-R-Q/K/R-K/R-R116 (129) at the C-terminus of the F2 protein and F (phenylalanine) at the N-terminus of the F1 protein, which can be cleaved by a ubiquitous set of host cell proteases located in the trans-Golgi membranes (130), and thus causing a systemic infection. In contrast, lentogenic strains carry the sequence 112G/E-K/R-Q-G/E-R116 and L (leucine) at residue 117 at the F protein cleavage site that can be properly processed by trypsin-like host proteases. The location of proteases (only in respiratory and gastrointestinal tracts of birds) restricts the spread of virus, and thus limits the virulence of the virus. The fusion process of NDV F protein differs from that of Influenza HA protein since it does not require slightly acidic pH for its activation and as a consequence the F protein fuses with the plasma membrane at neutral pH (131).

Other studies claim that cleavage of the F protein is not the only determinant of virulence. For example, some strains have multibasic cleavage sites, but exhibit low ICPI values, a property that is associated with the replication complex consisting of the NP, P and L proteins (132, 133).

1.4 The anatomy and physiology of avian digestive system

1.4.1 Avian digestive system organs and their functions

The avian digestive tract is a continuous tube, which consists of a mouth, esophagus, crop, proventriculus, ventriculus or gizzard, intestine, ceca, rectum, and cloaca (134).

1.4.1.1 Mouth

The mouth is the opening of the digestive tract. It consists of beak, tongue and oral cavity. The beak is a bony structure which is made up of upper and lower mandible. The roof of the mouth is made up of hard palate with a narrow slit in the center. The base of the mouth is the tongue. The function of this part is to pick up food and to push it to the next part of digestive tract (135, 136).

1.4.1.2 Esophagus and crop

Food is then passing through a muscular tube called esophagus, which locates to the right of the trachea. Many salivary glands line with the esophagus and secrete amylase to briefly hydrolyze the starch in the food. Most omnivorous and herbivorous bird species have an expansible sac along the esophagus known as crop. The crop does not only store and moisten food, but also serve as a functional barrier for pathogens and regulates the innate immune system. In some avian species, the secretions of the crop provide high energy nutrients for nestlings' growth (136, 137).

1.4.1.3 Stomach

After the esophagus and crop, the food then reaches the stomach of the bird. Birds have two stomachs, the proventriculus and the ventriculus. The proventriculus is the glandular stomach where digestion starts. It is smaller in granivorous species and larger in carnivorous and piscivorous species. The wall of the proventriculus includes a muscle layer, a glandular tissue layer, an areolar tissue layer and a mucous membrane. Unlike mammalian stomachs, the proventriculus has circular and longitudinal muscle layers but lacks an oblique muscle layer. The glands layer forms the largest part of the thickness of the wall (136). Generally, the gastric glands are distributed throughout the proventriculus, but they are not consistent among avian species. When food is present in the proventriculus, hydrochloric acid (HCl) and pepsinogen are secreted by oxynticopeptic cells which line the alveoli of the glands. Single glands group to form lobule, lobules group to form a common cavity and cavities further group to form a common duct. Ducts open into the luminal surface of proventriculus though the papillae, thus gastric fluid mixes up with food and starts the digestion (138).

The ventrculum or gizzard is a unique digestive organ in birds. A well-developed ventriculus is found in granivores, insectivores, and herbivores, but not in carnivores and piscivores. The wall of the ventriculus includes a tendinous connective tissue layer, a powerful circular and a longitudinal muscle layer, a submucosa and a glandular mucosa. The basal cells, chief cells, argyrophil cells, and epithelial cells of glands secrete a creamy-coloured, thick, tissue layer of glycoproteins that lines the inner surface of the gizzard. This koilin layer is hardened by the low pH of the gastric fluid and makes the surface rough like sand-paper. This layer also

functions as a protection of soft tissues from HCl, enzymes as well as mechanical damage. The gizzard contracts rhythmically up to four times per minute. Contents rub against the koilin layer and other particles in the gizzard, which reduces the size of particles. Small stones, grit particles or other hard material are found in the gizzard, which play a role as an abrasive source for the disintegration of food. The koilin layer is continuously renewed as it is worn by the grinding action (139).

The rather small volume of the proventriculus limits the retention time of food in it. The major digestive action of pepsinogen and hydrochloric acid takes place in the gizzard. Nevertheless, during contractions of gizzard, food contents refluxes into the proventriculus, and additional secretions from proventriculus are further added to the contents. The total retention time in the proventriculus and gizzard was estimated to be between half an hour and one hour (138).

The pH of the proventriculus and gizzard has been determined for different species and poultry under different feeding conditions. In general, the gizzard has a lower pH than the proventriculus. The pH of the duck´s proventriculus and gizzard is lower than that of chicken. The average proventriculus/gizzard pH values for broiler chickens having a normal pellet diet are reported to be between pH 3 and 4. But in some other avian species the average pH is higher, between 4.2 and 5.7 or lower between 1.6 and 2.3 (138, 139).

1.4.1.4 Intestine

When the particle size has been sufficiently reduced, the chyme then passes to the small intestine. The small intestine is a long tubular structure with multilayers including a serosal layer, longitudinal and circular muscle layer, submucosal layer, and mucosal layer (136).

The interior surface of the intestine is complexly folded into many structures called villi, which are long flattened, fingerlike projections, which greatly increases its surface area. On the apical surface of specialized epithelial cells of the villi are extensive projections called microvilli. There are two major types of cells lining the interior surface of the intestine, absorptive or principal cells and goblet cells. The absorptive cells are the most abundant. They are columnar epithelial cells with a large nucleus located basally and microvilli-covered luminal surface. Catabolic enzymes that are expressed by the cells break down molecules such that the cell can take them up. The goblet cells secrete copious mucous that cover the surface of villi to protect it from digestive enzymes and abrasion. Other cells, like enteroendocrine cells, Paneth cells, M cells, and intraepithelial leukocytes, scatters in the surface of intestine in small numbers. Between the villi are the crypts. Near the bottom area of the crypts, cells are rapidly dividing, then pushed up along the side of villi and differentiating into principal, goblet or other cells. In the interior of the villi, the lamina propria lies beneath the epithelial cells, which contains connective tissue, lymph vessels, capillaries, smooth muscle, nerve fibers and other tissues. The characters of the intestinal mucosal layer continue from the upper to the lower parts, with the fact that the villi get shorter and broader and crypts decrease in depth along the way, thus the thickness of intestinal mucosa decreases (140).

The small intestine is composed of the duodenum, jejunum and ileum. The duodenum can be easily distinguished by a "U" shaped loop next to the gizzard. There is no clear anatomical demarcation between the jejunum and ileum. The yolk sack residue which is called as Meckel’s diverticulum is usually referred to as the end of the jejunum (141).

The pancreatic juice produced by the pancreas and the bile produced by the liver are collected into ducts that open at the end of duodenum. Through gastroduodenal refluxes the chyme from

the gizzard is fully mixed with bile and pancreatic juices. The acidity of gizzard content is neutralized and the pH quickly rises above 6. The retention time in the duodenum is rather short, estimated to be less than 5 minutes. Jejunum and the ileum are suspended in the mesentery. Although the length of the jejunum and the ileum are approximately the same, the empty weight of the jejunum is usually higher than the ileum, 20 to 50%. Despite the shorter retention time in the jejunum (reported to be 40 to 60 minutes, which is approximately half of the ileum), digestion products from fat, starch and protein are to a large extent absorbed in this part of the small intestine. In the last segment of the small intestine, the ileum, water and minerals are absorbed (136).

1.3.1.5 Caeca

The small intestine ends in the ileo-cecal-colic junction, which is the junction of the ileum, caeca and the colon (also called large intestine or rectum). Avian caeca is found in various forms and sizes in different species and is absent in the others. The ceca are relatively large paired tubular structures in domestic fowl. From the junction to the blind sacs, the muscular and mucosal layers become thinner, the villi and ridges of epithelial cells become less and poorly developed. Together with urine and digestive fluids, small particles will be refluxed into the caeca, where salts and water will be reabsorbed. In some species, caeca work as fermenting chambers, in which the microbial digestion of cellulose and hemicellulose from tough vegetable food happen (136, 142).

1.3.1.6 Large intestine or colon

Compared to mammals, the large intestine is very short and smaller in diameter. It is very similar to the small intestine histologically, while the villi are shorter and richer in lymphoid follicles plus a thicker muscular layer. The colon is the last place of reabsorption of water and some electrolytes (136, 141).

1.3.1.7 Cloaca

The colon empties into the cloaca, a chamber where the urinary and reproductive systems also empty. The coprodeum receives faeces from the colon, while urinary and reproductive systems open into the urodeum. The coprodeum and urodeum are separated by a mucosal fold to prevent contamination from faeces to urinary and reproductive systems. The muscle layer of the cloaca is thicker than that of the intestine. From the colon entrance to the vent, the epithelium gradually changes from a columnar type to a cuboidal type and then to a stratified squamous type, and the villi gradually become broader and flatter until disappear. A special lymphoid organ called the bursa of Fabricius is located above the proctodeum of cloaca in young birds and disappears when the birds grow older (136).

1.4.2 Accessory digestive organs

1.4.2.1 Pancreas

The pancreas lies between the two arms of the duodenal loop. The secretions of this organ pass though ducts and open to the end of the duodenum via common papillaes shared with the ducts from the gall bladder and the liver. The pancreas is composed in most avian species of three lobes: dorsal, ventral, and splenic. The major functions of pancreas are producing pancreatic juice and hormones. The pancreatic fluid contains enzymes including amylase, chymotrypsinogen, trypsinogen, lipase, which further break down carbohydrates, proteins and lipids (143). In addition, pancreas secreted bicarbonate adjusts the pH of the small intestine to values between 6 and 7, the pH level at which the majority of digestive enzymes can function

efficiently. In addition to the production of digestive enzymes, the pancreas also produces hormones, including glucagon, insulin, somatostatin and others, which mix to the portal vein and play important role in regulating body metabolism and the functioning of the gut (144).

1.4.2.2 Liver and gall bladder

The liver locates in the anterior end of the birds' body cavity. It is divided into a larger right lobe and a smaller left one and in domestic fowl and turkey, the left lobe is divided into dorsal and ventral parts. Hepatocytes secret bile salts into the bile canaliculi that lead to the bile duct. The left bile duct directly leads to the duodenum while the right one lead to the gall bladder before it drains into the small intestine. The bile is mainly composed of water, electrolytes, bile acids, bile salts, neutral fats, bile pigments and some proteins and plays an important role as an emulsifier in fat digestion and absorption. Aside of fat metabolism, the liver is also involved in the metabolism of carbohydrate, protein, vitamins and minerals, storage of fat-soluble vitamins and some minerals, and phagocytosis of aged cells and pathogens (136, 145).

2 Aim of the study

Unlike human Influenza viruses that replicate in the respiratory tract and are airborne transmitted, avian viruses preferentially replicate in epithelial cells of the intestine, are excreted in high concentrations in feces and are transmitted via the fecal-oral route. The main glycoprotein of Influenza virus, hemagglutinin (HA) must be proteolytically cleaved into the N-terminal HA1 subunit and the C-terminal HA2 subunit in order to expose the fusion peptide after triggering by mildly acidic pH. On the fecal-oral route of transmission between avian species, the virus is exposed to the destructive fluids of the digestive tract, which are acidic and contain the proteases pepsin (gizzard) or chymotrypsin and trypsin (intestine). Since I wonder whether infectious virus particles can survive the passage through the gastrointestinal tract I mimicked it by incubating virus particles with stomach and gut fluids obtained from chickens. I quantified virus inactivation using plaque assays and integrity of the viral HA protein by western blotting.

In addition, since no cell line from the intestine of birds have been described I analyzed a new and unique gut epithelial cell line from chickens as a cell model for replication of Influenza virus and other avian pathogens. I investigated the morphology and growth of the cell lines and viral replication of five Influenza A, one Influenza B, one Influenza C and two Newcastle disease viruses in the various cell lines. I also tested the capability of these cells to process HA into its HA1 and HA2 subunit and to rescue Influenza virus with reverse genetic system.

3 Materials

3.1 Buffers and solutions

Buffer/Solution	Composition
PBS（phosphate buffer saline）	0.8% (w/v) NaCl, 0.02% (w/v) KCl, 0.02% (w/v) KH_2PO_4，0.135% (w/v) $Na_2HPO_4 \cdot 2H_2O$
PBST	0.1% Tween-20 in PBS
citrate buffer	0.1M citrate acid, 0.2M Na_2HPO_4
TNE buffer	50 mm Tris–HCl pH 7.4, 100 mm NaCl, 0.1 mm EDTA
Cell culture medium	DMEM, 10% (v/v) FCS, penicillin/streptomycin (100 units/mL)
Infection medium	DMEM, 0.1% (v/v) FCS, penicillin/streptomycin (100 units/mL)
Plaque assay overlay medium	1.25% (w/v) Avicel (FMC BioPolymer), 1% NaHCO3, 0.1% FCS and 2µg/ml TPCK-trypsin in 2x MEM
0.5% Crystal violet	0.5% (w/v) crystal violet in 25%(v/v) methanol and 75%(v/v) H_2O
0.05% Crystal violet	10% (v/v) 0.5% crystal violet in 4% (v/v) Formalin
Fixation solution	4% PFA (paraformaldehyde) in PBS
Stacking-gel	5% (w/v) acrylamide/bisacrylamide, 0.1% (w/v) SDS, 125 mM Tris·HCl (pH 6.8), 0.075% (w/v) APS, 0.15% (v/v) TEMED
Seperating-gel	12% (w/v) acrylamide/bisacrylamide, 0.1% (w/v) SDS, 375 mM Tris·HCl (pH 8.8), 0.05% (w/v) APS, 0.1% (v/v) TEMED
1x non-reducing loading buffer	62.5 mM Tris·HCl, 2% (w/v) SDS, 10% (v/v) glycerin, 0.01% (w/v) bromophenol blue, pH 6.8
1x reducing loading buffer	1x non-reducing buffer + 5% (v/v) β-Mercaptoethanol
Blocking buffer for western-blot	5% skimmed-milk powder in PBST
Blocking buffer for immunofluorescence	3% BSA in PBST

3.2 Consumables

Material	Manufacturer
PVDF (polyvinylidene difluoride) membrane	VWR
Cell culture flasks with filter cap, T25 T75 and T175	Sarstedt
Cell culture paltes, 12- and 6-well	Sarstedt
Pipettes, 5ml 10ml and 25ml	Sarstedt
Falcons, 15ml and 50ml	Sarstedt
Corning® Transwell® polyester membrane cell culture inserts	Sigma-Aldrich
Microscope slides and cover slip	VWR

VectorCell™ Trolox Antifade Reagent	Sigma-Aldrich

3.3 Kits and reagents

Material	Manufacturer
Phusion DNA Polymerase	Thermo Scientific
dNTP Mix 10mM each	Thermo Scientific
Enzymes: XhoI, BglII and buffer	NEB
T4 DNA ligase	NEB
GF-1 AmbiClean Kit (PCR&Gel)	vivantis
Invisorb Spin Plasmid Mini Kit	Stratec Biomedical AG
cOmplete™, EDTA-free Protease Inhibitor Cocktail	Carl Roth
Turbofect Transfection Reagent	Thermo Scientific
Lipofectamine® 3000 Transfection Reagent,	Thermo Scientific
ECLplus reagent	Pierce/Thermo
Collagen from rat tail	Sigma-Aldrich
pH strips, 2-9	Carl Roth
DMEM (Dulbecco's modification of Eagle's medium)	PAN
FCS (fetal calf serum)	PAN
BSA (Bovine serum albumin)	PAN
Opti-MEM	PAN
2X MEM (Minimal Essential Medium)	Biozym
Penicillin/streptomycin	Carl Roth
EDTA-trypsin	PAN
Furin inhibitor MI-701	Gift from PD. Stech
TPCK-trypsin	Sigma-Aldrich
TLCK-chymotrypsin	Sigma-Aldrich

3.4 Cells

Cells/Media	Manufacturer
Embryonated SPF eggs	VALO BioMedia
MDCKI and MDCKII (Madin Darby canine kidney cell)	ATCC CCL-34
CEF (Chicken embryo fibroblast cells)	prepared from 10-day-old embryos of white Leghorn hens.
Chicken intestinal epithelial cells (MM-CHIC CLONE 8E11, 9E6, 2GU, T3, T7, T12)	DSMZ (German Collection of Microorganisms and Cell Cultures GmbH)
Human embryonic kidney 293T cell	ATCC CRL-1573

Chicken erythrocyte	Labor Dr. Merk, Ochsenhausen

3.5 Viruses

Viruses	spieces	Source
Influenza A viruses		
A/FPV/Rostock/1934-M1 (H7N1)	avian	It contains the sequence PSKGR instead of PSKKRKKR at the C-terminus of HA1 (146)
A/duck/Bavaria/1/1977 (H1N1)	avian	Gift from PD. Stech
A/WSN/33 (H1N1)	human	
A/Panama/2007/1999 (H3N2)	human	
A/New Caledonia/2000/1999 (H1N1)	human	
Influenza B virus		
B/Lee/40	human	
Influenza C virus		
C/JJ/50-NS of C/JHG/66	human	
Newcastle disease virus		
Italien	avian	

3.6 Apparatuses

Apparatuses	Manufacturer
Cell culture incubator	Heraeus
Centrifuge 5417R	Eppendorf
Ultralcentrifuge	Beckman
SW 32Ti Roter	Beckman
NanoDrop 1000 Spectrophotometer	Thermo Scientific
Power Pack P25	Biometra
Semidry membrane blotting machine	Peqlab
Fusion SL camera system	Peqlab
PCR	Biometra
CASY® cell counter	Roche
Inverted microscope	Motic AE30
Axio Vert.A1 fluorescence microscope	Zeiss
Live cell imaging with VisiScope confocal FRAP System	VisiScope system
Thermo cycler	Eppendorf

3.7 Plasmid and primers

Purpose	Name/Sequence
Reverse genetics (FPV M)	PB1, PB2, PA, HA, NP, NA, M, NS-pHH21 Exp-PB1, Exp-PB2, Exp-PA, Exp-NP-pcDNA
Expression of HA with monobasic cleavage site	monoHA-pCAGGS
Expression of HA with polybasic cleavage site	polyHA-pCAGGS
HA sense	5'CCGCTCGAGATGAACACTCAAATCCTGG3'
HA anti-sense	5'GAAGATCTTTATATACAAATAGTGCACCGC3'

3.8 Antibodies

Antibodies	Source
rabbit monoclonal antibody against FPV-HA2	Gift from Dr. Klenk
mouse monoclonal antibody against β-Catenin	Sigma- Aldrich
HRP anti-rabbit antibody	Sigma-Aldrich
goat anti-mouse IgG-Alexa 488	ThermoFisher

4 Methods

4.1 Cell culture

4.1.1 Continuous cell culture

MDCK II, chicken intestine epithelium 8E11, 9E6, 2GU, T3, T7 and T12 cells, as well as human embryonic kidney 293T cells are cultured in complete culture medium (DMEM supplemented with 10% FCS, 100 units/ml penicillin and 100 µg/ml streptomycin) at 37 °C and 5% CO_2. Cells are split when they reach 90-100% confluence. After washing the cell monolayer with PBS, EDTA-trypsin was added to detach the cell monolayer from the cell culture flask. Once cells were rounded and lifted, fresh medium was added to stop the trypsin activity. Pipette repeatedly to fully suspend the cells and avoids cell clumps.

4.1.2 Chick embryo fibroblasts (CEF) preparation

CEF were prepared with specific pathogen-free 10-day old embryos as described before. Briefly, egg with healthy embryo was cleaned with 70% ethanol and opened with sterile scissors. After removal of the membrane, the embryo was gently and slowly pulled out with sterile forceps. The head, wings, feet, and body cavity contents were dissected from the embryo, and the remaining part was washed with PBS and dissected by sharp scissors. Add 37°C prewarmed trypsin solution and shake gently at 37°C for 15 to 20 min in order to obtain separated single cell. Centrifuge 10 min at 500×g, remove the supernatant and resuspend the cell pellet with fresh complete culture medium to get an evenly distributing cell suspension. Aliquot of cell was seeded in cell culture flask and kept at 37°C and 5% CO_2.

4.2 Virus propagation, purification and titration

4.2.1 Virus propagation in cells

Influenza A strains, A/FPV/Rostock/1934-M1 (H7N1), A/duck/Bavaria/1/1977 (H1N1), A/WSN/33 (H1N1), A/Panama/2007/1999 (H3N2), A/New Caledonia/2000/1999 (H1N1) and Influenza B strain B/Lee/40 were propagated with MDCKII cells, recombinant Influenza C strain C/JJ/50 with NS of C/JHG/66 grows in MDCKI cells, while NDV Italian strain was propagated with CEF cell.

Cells at 90% confluence were infected with viruses at proper moi, 0.0001 for Influenza A and NDV, 0.001 for Influenza B and 0.01 for Influenza C, respectively. After one-hour incubation at 37°C, the supernatant was replaced by fresh infection medium (DMEM with 0.1% FCS, penicillin/streptomycin (1% each) containing TPCK-trypsin at a final concentration of 2µg/ml) and cell cultures were further incubated at 37 °C (33°C for Influenza C) until most cells were dead. The cell supernatant was collected, cleared (10 min at 5000xg) and viruses were titrated, aliquoted and stocked at -80°C.

To create avian Influenza virus preparation with uncleaved HA MDCKII or 8E11 cells were infected with avian strains A/FPV/Rostock/1934-M1 (H7N1) or A/duck/Bavaria/1/1977 (H1N1) at a moi of 1 respectively and incubated in infection medium without TPCK-trypsin for 12 hours. The cell supernatant was collected and cleared (10 min at 5000xg).

Both A/FPV/Rostock/1934-M1 (H7N1) and A/duck/Bavaria/1/1977 (H1N1) with cleave HA and with uncleaved HA were pelleted at 29000 rpm and 4°C for 2 hours in a SW 28 rotor, dissolved in 100 µl TNE buffer and stored in aliquots at -80°C.

4.2.2 Virus propagation in chicken embryo

Specific-pathogen-free (SPF) eggs from VALO BioMedia were used for Newcastle disease virus propagation. The embryonated chicken eggs were kept in 37°C till 9 or 10 days. The inoculation point which is 0.5 cm above air sac circle and should avoid obvious blood vessels was marked when candling. 10^4 pfu (plaque forming unit) of virus (100-300µl) was injected though a hole in the inoculation point into the allantoic cavity with syringe and needle. Then the holes were sealed with wax and the eggs were kept in 37 °C incubator. Candling eggs for embryo death since 24 hours post inoculation. Eggs with dead embryo were chilled at -80°C for 20min. Finally, the clear allantoic fluid from infected egg were collected, cleared (10 min at 5000xg) and stored at -80°C for further use.

4.2.3 Virus titration

4.2.3.1 Plaque assay

Cells were seeded in 6 well plates to reach 90% confluence the next day. Virus samples were serial tenfold diluted with infection medium, and 500µl of each dilution were loaded into one well. After 1 hour incubation at 37 °C with shaking every 15 minutes, cells were washed with PBS and overlayed with overlay medium, After incubation for 48 h at 37 °C the overlay medium were washed away and cell cultures were fixed with 4% PFA and stained with 0.1% crystal violet, and the plaques were counted.

4.2.3.2 Hemagglutinin assay

50 µl PBS was added in each well of a 96 well U-bottom microwell plates. 50 µl virus sample was added in each well of the first column and serially twofold diluted by pipetting with multichannel pipette. Throw away 50µl from the second last column and keep the last column only PBS as a control. 50µl 1% chicken red blood cells were added in each well and results of hemagglutinin were recorded after 30 minutes of incubation at room temperature.

4.3 Mimic Influenza virus passing through chicken digestive tract

4.3.1 Chicken digestive tract fluid collection

Six and two healthy chickens (*gallus gallus*, 20 weeks old, hatched from VALO BioMedia SPF eggs and raised under SPF conditions) were sacrificed. Ligations were made at the beginning and the end of the gizzard and at the end of the small intestine (duodenum). Fluids from the gizzard (~10 ml) and intestine (~6 ml) were collected, combined and passed through 0.2µm filters. The pH of the combined gizzard fluids and gut fluids was measured with pH test strips to be 3.5 and 6.5, respectively. Aliquots of both fluids were stored at -80°C until use.

4.3.2 Avian Influenza virus with uncleaved HA incubation in gizzard or gut fluid

Chicken gizzard fluid and gut fluid were diluted with citrate buffer at different ratios, 1:3, 1:10, 1:30, 1:100, 1:1000. Citrate buffer at pH 3.5 and 7 were used for gizzard fluid dilution, while citrate buffer at pH 6.5 was used for gut fluid dilution.

In each experiment 10µl concentrated avian Influenza A virus with uncleaved HA (~$5x10^6$ PFU) was incubated with 60µl undiluted or diluted gizzard or gut fluid at 42°C for 20 minutes. Bovine serum albumin solution (PAN, Aidenbach, Germany) were added or not to a final concentration of 1µg/µl. After the incubation, 10µl virus and buffer mixture were used for western-blot and the remaining 60µl were immediately diluted with infection medium and virus titers were determined by plaque assay.

While our goal is to investigate virus activation by gizzard/gut fluid thus further virus activation by additional trypsin should be prevented, in this case, virus incubated with gizzard or gut fluid,

trypsin was not present in the infection medium when performing plaque assay. And trypsin was also excluded from the overlay medium. Instead, 5 hours post infection, a second layer of overlay medium containing 2 µg/ml TPCK-trypsin was added to activate progeny virus and allow plaque formation.

4.3.3 FPV M1 virus with uncleaved HA incubation in buffer of different pH or different concentration of TPCK-trypsin and TLCK-chymotrypsin.

Sodium acetate-acetate buffers adjusted to pH 3, 4, 5, 6 or 7 were prepared and sterile. Also, TPCK-treated trypsin or TLCK-treated chymotrypsin was dissolved in PBS at a final concentrations of 2000 µg/ml, 200 µg/ml, 20 µg/ml or 2 µg/ml respectively. 10 µl concentrated FPV M1 virus with uncleaved HA was added in 60 µl buffer of different pH values or different concentrations of protease. After incubation at 42°C for 20 minutes, western-blot and plaque assay were performed.

4.3.4 SDS-page and western-blot

After the incubation 10µl FPV M1 virus and buffer mixture was removed from each sample, reducing SDS-page buffer (10 µl) was added, samples were boiled at 95°C for 10 minutes and 20 µl of sample/loading buffer mix was loaded in 12% sodium dodecyl sulfate-polyacrylamide gels (SDS gel). Electrophoresis was done in a sequential manner, ie 80V for 30min followed by 1 hour at 160V. Then polyacrylamide gels were blotted onto polyvinylidene difluoride (PVDF) membrane with 220mA for 70 minutes. After blocking of membranes (blocking solution: 5% skim milk powder in PBS with 0.1% Tween-20 (PBST)) for 1 h at RT, anti HA_2 antibodies (diluted 1:2000 in blocking solution) were applied overnight at 4°C. After washing (3x10 min with PBST), horseradish peroxidase-coupled secondary antibody (anti-rabbit, Sigma-Aldrich, Taufkirchen, Germany, 1:5.000) was applied for 1 hour at RT. After washing, signals were detected by chemiluminescence using the ECLplus reagent (Pierce/Thermo, Bonn, Germany) and a Fusion SL camera system (Peqlab, Erlangen, Germany).

4.4 Characterization of chicken intestinal epithelium cell

4.4.1 Cell growth curve

In order to evaluate growth properties of the chicken intestinal epithelial cell line under a given set of culture conditions, the growth curve of cell counts after subculture was constructed. CHIC 8E11cells at passage 90 or CHIC T12 at passage 27 were used. 1.5 $x10^5$ cells were seeded in each well of a 12-well culture plate. Cells from three wells were detached and counted every 12 hours by CASY® cell counter (Roche, Mannheim, Germany) according to manufacturer instructions. 10 µl of freshly resuspended cell samples were diluted in 10 ml system dilution liquid called CASY®ton and measured by the device. Cell numbers and viability are given. Cleaning of the machine before and after each measurement is required. The experiment lasts until the cells are confluent in the well. The doubling time (DT) was calculated with the following formula: TD = t (lg2 / lgNt-lgN0). t represents duration of cell culture, while N0 represent cell number of inoculation and Nt represent cell number after culturing for t hours.

4.4.2 Virus growth kinetics

To assess virus multistep growth kinetics, cell monolayers of 8E11 and T12 were infected with Influenza virus or Newcastle disease virus and MDCK or CEF were used for comparisons. According to virus virulence, different moi were used for different viruses as shown in Table 5.1 . After 1h adsorption, cells were washed with PBS, the supernatant was replaced by 3 ml

fresh infection medium without or with TPCK-trypsin (1µg/ml). 200 µl supernatant was harvested after a defined incubation time, cell debris were cleared by a centrifugation at 5000xg for 10 min. Supernatants were stored at -80°C for titration. For experiments with TPCK-trypsin, fresh TPCK-trypsin was added every 48 hours. Collected virus samples were titrated by HA- and plaque assay. Two or three independent experiments were done.

4.4.3 Plaque formation and plaque size measurement

To figure out whether Influenza viruses and Newcastle disease virus can form plaques in the chicken epithelial cell monolayer in presence of overlay medium, 8E11 cell were seeded in 6-well-plates (approximately $1.2x10^6$ /well) to reach 90% confluency the next day. MDCKII and CEF cells were used for comparisons. A/FPV/Rostock/34, A/WSN/33, NDV Italien of known titers were diluted and used to infect cell monolayer. Plaque assay was performed as described in 4.2.3.1. 2 days and 3 days post infection, the overlay medium were washed away and cells were fixed and stained with 0.1% crystal violet. Images of 50 randomly selected plaques per virus-cell combination were taken, and plaque areas were determined using the ImageJ software (NIH) and converted into plaque diameters. Then the plaque diameters were normalized to that in MDCKII or CEF cells.

4.4.4 Expression of Influenza HA protein in CHIC 8E11 cell

4.4.4.1 Plasmids construction

The full length HA genes from FPV M1 or wt with either monobasic or polybasic cleavage site was amplified from plasmid pHH21. For the PCR, the following regent were mixed thoroughly (left) and then the PCR was performed as following program (right):

Component	Amount
5×Pusion HF buffer	10 µl
Template (pHH21-poly/monoHA)	100 ng
10mM dNTPs	2 µl
Phusion polymerase	0.5 µl
10 µM Primer-F	2 µl
10 µM Primer-R	2 µl
ddH_2O	to 50 µl

Cycle step	Tm	Time	Cycles
Step1	98°C	30s	1
	98°C	10s	
Step2	55°C	30s	30
	72°C	45s	
Step3	72°C	10min	1
	16°C	hold	

PCR products were load to agarose gel and purified by kit. Concentration of purified PCR product were determined by Nanodrop.

For double enzyme digestion, the following regent were mixed thoroughly:

Component	Amount
10×NEBuffer	5µl
XhoI	1µl
BglII	1µl
DNA	1µg
ddH_2O	to 50µl

poly/mono HA and expression vector pCAGGS were used as DNA template. Mixed reactions were incubated at 37℃ for 2 hours. Products were loaded in agarose gel and purified by kit. Nanodrop was used to measure the concentration.

Then for ligation of double digested HA to pCAGGS, the following regent were mixed thoroughly:

Component	Amount
HA DNA	50ng
pCAGGS DNA	100ng
T4 ligase	1μl
10×T4 DNA ligase buffer	2μl
ddH2O	to 20μl

Well-mixed ligation reaction system was incubated at 16℃ overnight. On the second day, thaw competent cells on ice, and then add 1 μl 100 ng/μl pCAGGS-monoHA or pCAGGS-polyHA plasmid into 100 μl E. coli competent cell and mix gently by pipetting up and down. Place the mixture on ice for 30 min then heat shock at 42°C in water bath for 45 seconds. Place mixture on ice for at least 2 min then add 900 μl antibiotic free LB mediato the tube and shake the tube at 37°C for 60 minutes at a speed of 200 rpm. Spread 50–100 μl of the cells onto the plates containing 100 μg/ml Ampicillin. Incubate the plates at 37°C overnight. On the next day, pick up single colony into 100 ml LB media containing 100 μg/ml Ampicillin and shake at 37°C for 22 hours at a speed of 200 rpm. Pellet cells at 5,000 × g for 10 minutes then discard the supernatant.

Plasmids were extracted from the bacteria cells by kit following the instruction of manufacturer. In brief, cell pellet is resuspend thoroughly in 12ml of Cell Resuspension Solution by vortexing or pipetting. Add 12ml of Cell Lysis Solution. Invert gently 3–5 times to mix then incubate for 3 minutes at RT. Add 12ml of Neutralization Solution and Invert gently 10–15 times to mix. Centrifuge the lysate at 14,000 × g for 20 minutes at RT using a fixed angle rotor. Finally, the concentration of the plasmids was measured by analyzing the absorbance at 260nm with a NanoDrop spectrometer.

4.4.4.2 Transfection of cells

After concentration determination, 4μg plasmid DNA was transfected with TurboFect into 8E11 cells in a well of 6-well-plate as described by the manufacturer (Thermo Fisher Scientific, Carlsbad, United States). Briefly, cells were prepared to reach 80% to 90% confluency, washed and change into fresh culture medium before transfection. 4μg plasmid was diluted with 400μl Opti-MEM. 4 μl transfection reagent was added in the diluted DNA and mix immediately vortexing. Incubate the transfection reagent/DNA mixture for 20 minutes at RT, followed by adding 400μL of it drop-wise to each well. Then cells were put back to 37°C incubator. Medium change was needed or not in between.

For the furin inhibition experiments, the peptidomimetic drug MI-701 (added from a 2 mM stock solution dissolved in H_2O) was added 1 hour after transfection to give final concentrations of 25 to 150 μM.

4.4.4.3 HA protein detection

24 hours post transfection cells were washed with ice-cold PBS, collected in 1.5ml Eppendorf tubes and pelleted at 5000xg for 10 minutes. Cell pellets were lysed in 100 µl 1% NP-40 in PBS for 20 minutes on ice. Lysates were cleared (10 min at 5000xg) and a 20 µl aliquot of the supernatant was analyzed by western-blotting with anti-HA_2 antibody as described in 4.3.4.

4.4.5 Generation of FPV M1 virus by reverse genetics

Reverse genetics was performed as previously described (34). 293T and 8E11 cells were grown to 100 % confluence in a T75 flask and then trypsinized with trypsin-EDTA and resuspended in 10 ml culture medium. Cells were counted and seeded into 60mm cell culture dishes (3 ml per well with $4.5x10^6$ 293T cells/ $2.7x10^6$ 8E11 cells/ $2x10^6$ 293T plus $1.5x10^6$ 8E11 co-culture). On transfection day, twelve pPMV plasmids, which contain eight FPV M1 virus gene fragments and four protein expression plasmids, were mixed in 800µl serum- free Opti-MEM medium (0.05 µg of PA expression plasmid and 0.5 µg of all other plasmids). Then cells were transfected with plasmids mixture with TurboFect reagent according to the manufacturer's instructions. Six hours post transfection, cells were washed twice with PBS and added with 3 ml infection medium with TPCK-trypsin at a final concentration of 1µg/ml. Then incubate the cells at 37°C. 2 days after transfection, supernatants were collected as the P0 generation of rescued viruses. 90% confluent MDCK II cells in T25 cell culture flask were infected with 1ml above supernatant then maintained in 3ml infection medium with 2µg/ml TPCK-trypsin. 2 d.p.i, the supernatant was collected as the P1 generation of virus.

4.4.6 Cell polarization

4.4.6.1 Cell culture preparation

Transwell permeable filters (Corning, 12 mm filters with 0.4 µm pores in 12-well-plate) were used for chicken intestinal epithelium cell polarization attempt. The filters were coated with 1.5 µg/ml collagen solution and solidify at 37°C overnight. Add 500µl and 1.5ml cell culture medium to apical and basolateral compartments of the transwell filter, respectively. And pre-incubate the plates at 37°C for at least 30 minutes. Seed 1.5×10^5 cells in 500 µl complete culture medium onto the membrane filter and keep the plate in 37°C. Check the cell growth under light microscope and change medium daily. Once the cells are confluent on the membrane, change the apical medium into DMEM with 5% FCS while keep the FCS concentration in the basol chamber to facilitate cell polarization.

4.4.6.2 Indirect immunofluorescence staining of adherens junction protein

3, 5, 7 days after seeding 8E11 and MDCKII cells onto Transwell filter, the cells were washed 5 times (5min each) with PBS and fixed with 4% paraformaldehyde (PFA) for 20 min. Then the filters were carefully cut out from the insert frame and adherens junction protein β-Catenin was stained by IFA. The cells were blocked with 3% BSA for 30 minutes and then incubated with primary antibody, i.e. mouse monoclonal antibody against β-Catenin (Sigma, 1:500 diluted in 3% BSA). Again wash with PBS (5 times 5min each time), and secondary fluorescent antibody goat anti-mouse IgG-Alexa 488 (10 µg/ml) were added and the cell culture plate was incubated at RT for 1 hour avoiding light. Followed by another washing step, cell nucleuses were stained with DAPI (Sigma,1:5000 diluted with PBS) for 10 minutes. Then the filters were placed on microscope slide with the apical surface facing up. The mounting solution VectorCell™ Trolox Antifade Reagent was evenly distributed onto the filter, and the filters were carefully covered with cover slip. Let the mounting solution dry in dark at RT overnight and then images were

visualized using VisiScope confocal FRAP System. Images were taken with 0.5 μm increments of Z-stacks and images were analyzed with Image J software.

5 Results

5.1 Virus survival in digestive fluid

5.1.1 Virus activation by gizzard fluid

Fluid from the gizzard of six chickens were squeezed out, combined and filtered. The fluid exhibits a pH of 3.5, which agrees with published data (139). The mutant M1 of fowl plaque virus (A/FPV/Rostock/34, H7N1) and a duck isolate (A/duck/Bavaria/1977, H1N1) were used. First I prepared viruses with uncleaved HA by infecting cells at a high multiplicity of infection (moi) and incubated for ~12 hours in the absence of trypsin. Then the supernatant was concentrated by ultracentrifugation at 29000 rpm for two hours.

For FPV M1, western blotting with HA2 specific antibody showed that the virus preparations contained mainly uncleaved HA_0 and plaque assay revealed a titer of ~$8x10^5$ pfu/ml. After activation by incubating with 2 µg/ml trypsin, HA was completely cleaved and virus titers increased to $5x10^8$ pfu/ml, i.e. around 600 fold (Fig. 5.1A), which is in agreement with published studies (147, 148).

To mimic the virus passage through the gizzard, 10 µl concentrated virus ($5x10^6$ infectious particles after trypsin activation) was mixed with 60 µl of serial dilutions of gizzard fluid, which was adjusted with citrate buffer to pH 3.5. Well-mixed samples were incubated at 42°C (the body temperature of birds) for 20 minutes and then neutralized with medium and treated with trypsin to activate HA. However, we were not able to detect a single infectious virus particle in a plaque assay, even at the highest dilution of 1:1000 (Fig.5.1A).

The destructive effect of the gizzard fluid on virus infectivity might be due to its acidic pH. It is well documented that Influenza viruses having a cleaved HA are inactivated at slightly acidic pH between 5.2 and 6, since the acid treatment triggers HA to execute the irreversible conformational change that catalyzes membrane fusion (110). Since uncleaved HA is not able to perform this conformational change we asked whether they are more stable under acidic conditions. $5x10^6$ infectious particles of FPV M1 were incubated with buffer adjusted to a pH between 3 and 7. No plaques were detected after incubation at pH 3 and pH 4, the infectivity was greatly reduced to $5x10^5$ plaques, i. e. by 90% at pH 5, but was only marginally affected at pH 6 (Figure 5.1B). Thus, virus particles with uncleaved HA are more stable as particles having a cleaved HA, as described before (149), but are (almost) completely inactivated at the pH of the chicken gizzard.

The gizzard fluid contains the protease pepsin. We therefore tested the integrity of virus particles after the incubation with gizzard fluid by western blotting using antibodies against the HA2 subunit. Undiluted gizzard fluid almost completely degrades HA, only one band with a molecular weight lower than authentic HA2 remains. At 1:10 and 1:30 dilutions two bands running above and below the 36 kDa size marker were detected. Only at a high dilution of 1:100 and 1:1000 HA remains mainly undigested (Fig.5.1C). We repeated this experiment with combined gizzard fluids from two other chickens and added the protein albumin to a high final concentration (1 µg/µl) to better mimic virus uptake by food. However, even at a dilution of 1:1000 no virus infectivity remains (not shown), and degradation of HA was only marginally retarded by the presence of albumin (Fig. 5.1D).

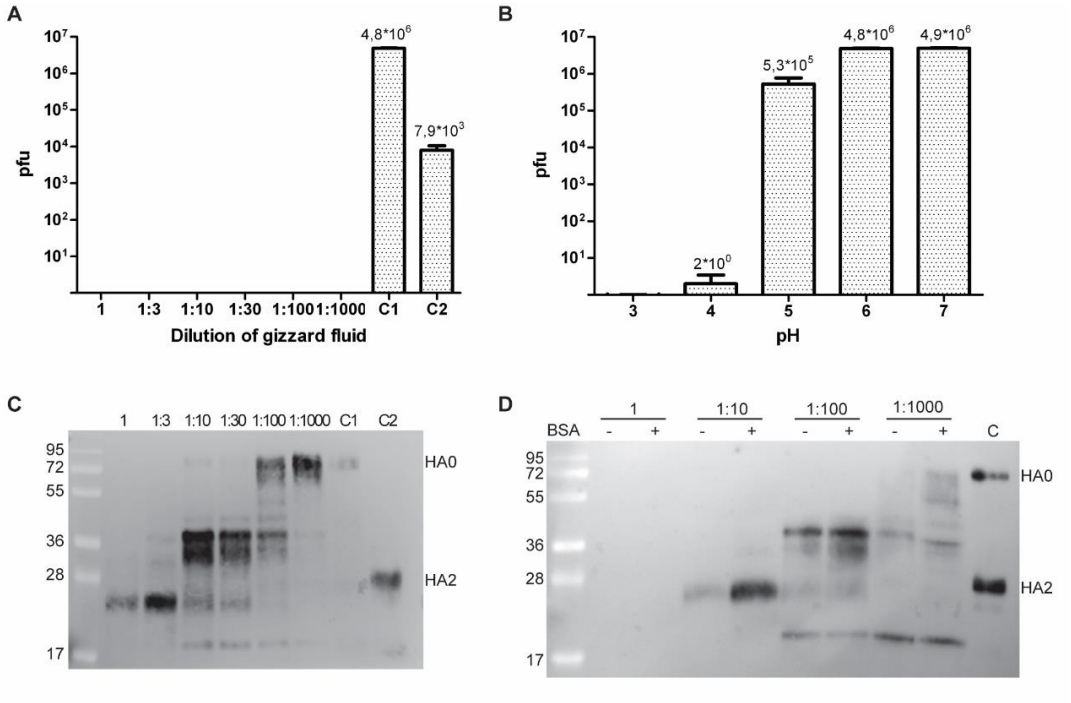

Fig. 5.1: Influenza virus is inactivated in gizzard fluid by low pH and proteolysis

(A) Fowl plaque virus M1 (H7N1) containing HA with a monobasic cleavage site was grown in the absence of trypsin and pelleted from cell culture supernatants. 10 µl of the preparation was incubated for 20 minutes with serial dilutions of gizzard fluid and then activated with trypsin (20µg/ml). Viral titers were determined with a plaque assay. C1: 10 µl only activated with trypsin. C2: 10 µl of the preparation.

(B) 10 µl of the virus preparation was incubated for 20 minutes with buffer adjusted to pH values between 3 and 7 and the plaque titer was determined. The mean of three different incubations including standard deviation is shown is shown in A+B. Numbers indicate the size (kDa) of molecular weight markers.

(C) Aliquots of the samples from A were subjected to SDS-PAGE and Western blot using antisera against the HA_2 subunit. Controls: virus particles with uncleaved (C1) and cleaved HA (C2) as size marker for the SDS-PAGE mobility of HA0 and HA2, respectively.

(D) FPV M1 was incubated with serial dilutions of gizzard fluid without (-) or with (+) 1µg/µl BSA (1µg/µl) for 20 min. Samples were then subjected to SDS-PAGE and Western blot using antisera against the HA_2 subunit. C: virus particles with partially cleaved HA as size marker for the SDS-PAGE mobility of HA0 and HA2. No virus infectivity was detected if an aliquot of each sample was analyzed in the plaque assay.

Since acidic pH inactivates virus, we further questioned whether viruses are more resistant in gizzard fluid diluted with buffer adjusted to neutral pH, mimicking virus uptake by drinking of water. The gizzard fluid was serially diluted with citrate buffer of pH 7, and again, 10 µl concentrated virus was incubated with the serial dilutions at 42 °C for 20 minutes.

In this set of experiments, we did not treat virus particles with trypsin after incubation with the gizzard fluid to determine whether it might contain a protease that activates HA. Similar to the previous experiments undiluted gizzard fluid completely inactivates virus particles (Fig. 5.2A). Interestingly, the result from the incubations with diluted gizzard fluid is quite different. At a dilution of 1:3 virus titers were reduced by only ~50%, i.e. from $1x10^4$ to $5x10^3$. At higher dilutions (1:10, 1:30 and 1:100), the infectivity of the virus preparation even increased to ~$2x10^6$,

which is similar to treatment with trypsin, suggesting that the gizzard fluid contains a trypsin-like protease, which activate virus by cleaving HA0 to HA2. Western blotting using antibodies against the HA2 subunit (Fig. 5.2B) supports this assumption. Bands with the size of HA2 and smaller appear when virus particles were incubated with various dilutions of gizzard fluid, which are highly similar to the bands obtained by trypsin-treatment. A likely explanation would be that pepsin, the main protease of the gizzard, which has an optimum pH of ~2; but becomes inactive at pH 5 and thus does not digest if the fluid is diluted with neutral buffer. Instead, another unknown trypsin-like protease becomes active at neutral pH that activates HA.

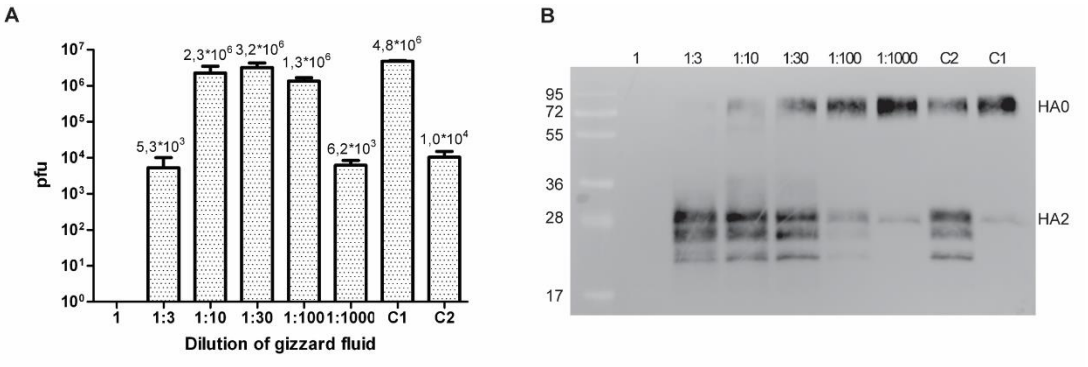

Fig.5.2: Incubation of FPV with gizzard fluid diluted with neutral buffer

(A) FPV M1 (10 µl) was incubated for 20 minutes with 60 µl gizzard fluid serially diluted with buffer adjusted to pH 6.5. In contrast to experiments shown in Fig.5.1 samples were then not treated with trypsin. Viral titers were determined with a plaque assay. C1: 10 µl virus activated with trypsin. C2: 10 µl of the virus preparation not treated with trypsin. The mean of three different incubations including standard deviation is shown.

(B) Aliquots of the samples from A were subjected to SDS-PAGE and western blot using antisera against the HA2 subunit. Controls: virus particles with uncleaved (C2) and cleaved HA (C1) as size marker for the SDS-PAGE mobility of HA0 and HA2, respectively. Numbers indicate the size (kDa) of molecular weight markers.

Furthermore, I performed the same experiments with a LPAIV strain (A/duck/Bavaria/1977) which was isolated from cloacal swabs of a mallard duck (150). I prepared concentrated virus particles with uncleaved HA. 99.9% of the virus HAs remain uncleaved, whereas virus titers increased from $2x10^3$ to $2x10^6$ by treatment with trypsin. Undiluted gizzard fluid completely inactivated A/duck/77 as well, but gizzard fluid diluted with neutral buffer activates viral infectivity at all dilutions, almost to the same extent as trypsin treatment (Fig. 5.3). Compared to FPV M1 which can be fully activated at incubation with 1:10 to 1:100 diluted gizzard fluid, A/duck/77 is completely activated at lower dilutions and thus more adapted to infection via the gastro-intestinal tract.

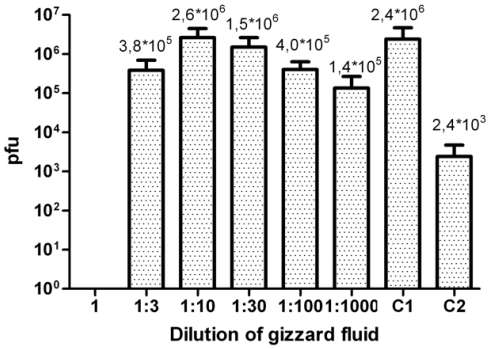

Fig.5.3: Incubation of A/duck/77 with gizzard fluid diluted with neutral buffer

A preparation of avian virus A/duck/77 (10 µl) was incubated for 20 minutes with 60 µl gizzard fluid serially diluted with buffer adjusted to pH 6.5. Viral titers were determined with a plaque assay. C1: 10 µl virus activated with trypsin. C2: 10 µl of the preparation not treated with trypsin. The mean of three different incubations including standard deviation is shown.

In sum, gizzard fluid, when diluted with buffer of pH 3.5, even at a dilution of 1:1000 and enriched with additional protein, quantitatively inactivates Influenza virus particles due to its acidic pH and proteolytic digestion of HA and probably of other viral proteins. However, when diluted with buffer at neutral pH, gizzard fluid activates Influenza virus particles, suggesting that a trypsin-like protease becomes active at neutral pH. And the duck isolate is completely activated at lower dilutions of the gizzard fluid compared to FPV M1, which indicate a better adaption of this strain to infect via the gastro-intestinal tract.

5.1.2 Virus inactivation by intestine fluid

Since the digestive fluid of the intestine contains trypsin and chymotrypsin, I wondered whether they can serve as a source for enzymes that cleaves monobasic HA of LPAIV. First I tested the effect of a wide concentration range of trypsin on titers of a FPV M1 preparation (10 µl) in the absence of trypsin. Every tested concentration of trypsin activates the virus ~100 fold, i. e. virus titers increased from $2x10^4$ to $2.5 x10^6$ (Fig. 5.4A). Western-blotting with an aliquot of the incubation showed that the two lowest concentrations of trypsin (2 and 20 µg/ml, which are usually used in plaque assays and multiple step growth experiments) cleaved ~ 50% and 100%, respectively, of HA into its subunits. At higher concentrations an additional band with a molecular weight clearly lower than genuine HA2 appeared, indicating that the protease is beginning to cleave other residues in HA, but this apparently does not affect the infectivity of the virus preparation as a whole (Fig. 5.4B).

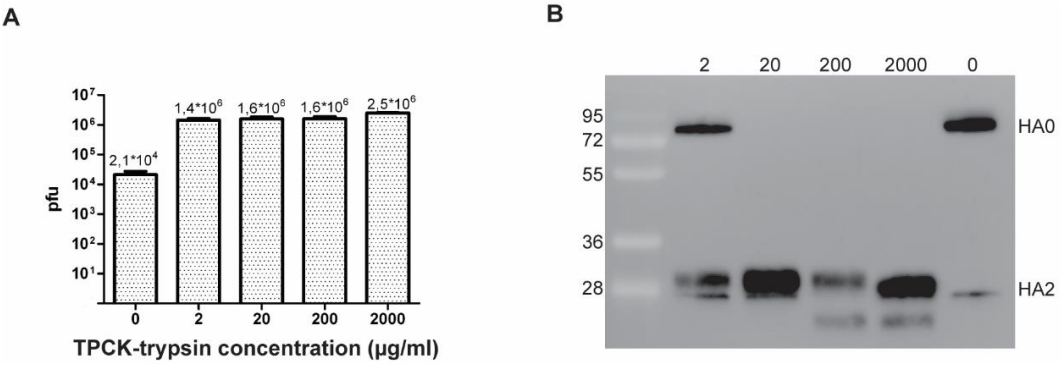

Fig.5.4: Incubation of FPV with TPCK-trypsin

FPV M1 was incubated with the indicated concentration of trypsin for 20 min. Aliquots of samples were then subjected to plaque assays**(A)** or to SDS-PAGE and western blot using antisera against the HA2 subunit **(B)**.

Then I tested the effect of serial dilutions of gut fluid on virus activation and integrity of HA. Fluid from the first part of the gut (mainly duodenum) of six chickens was collected and then serially diluted with citrate buffer of pH 6.5, which is the pH of the gut fluid and doesn't destroy virus infectivity. Again, 10 µl concentrated virus was incubated with the serial dilutions at 42°C for 20 minutes. Only at a dilution of 1:1000 the virus preparation having an uncleaved HA was activated ~10fold, i.e. an increase in virus titer from $3x10^4$ to $2x10^5$ was observed (Fig. 5.5A). Since trypsin treatment (2 µg/ml) caused an increase in viral titers to $5x10^6$ it can be calculated that ~10% of potentially infective virus particles were activated by the gut fluid. Western blotting showed that only a small fraction of HA0 was processed into functional HA2, most bands detected by the antiserum had a higher molecular weight suggesting HA cleavage at amino acids other than the authentic cleavage site. The same two HA degradation products prevail in less diluted gut fluid whereas undiluted fluid almost completely degraded HA (Fig. 5.5B). Since the pattern of HA bands is different from that obtained with viruses incubated with high concentrations of trypsin it indicates that other enzymes, such as chymotrypsin, also digest the virus particles. This increasing degradation of HA is reflected by a decrease of the virus titers. At a dilution of 1:100 no virus particles were activated, i.e. the virus titer is slightly lower ($1.3x10^4$) compared to samples not treated with trypsin ($2.8x10^4$). At lower dilutions of gut fluid the residual viral infectivity is further diminished; after incubation with undiluted gut fluid 95% of virus particles are inactivated. However, in contrast to experiments with the gizzard fluid ~ 2000 virus particles remained infectious after incubation with gut fluid.

I repeated this experiment with combined gut fluids from two other chickens and added the protein albumin at a high final concentration (1 µg/µl) to better mimic digestion of food in the duodenum. Nevertheless, essentially the same result was obtained. The presence of albumin had a slightly beneficial effect on virus titers, especially at the dilution of gut fluid of 1:10, but HA was still degraded to similar extent compared to samples not supplemented with albumin (Fig. 5.5CD).

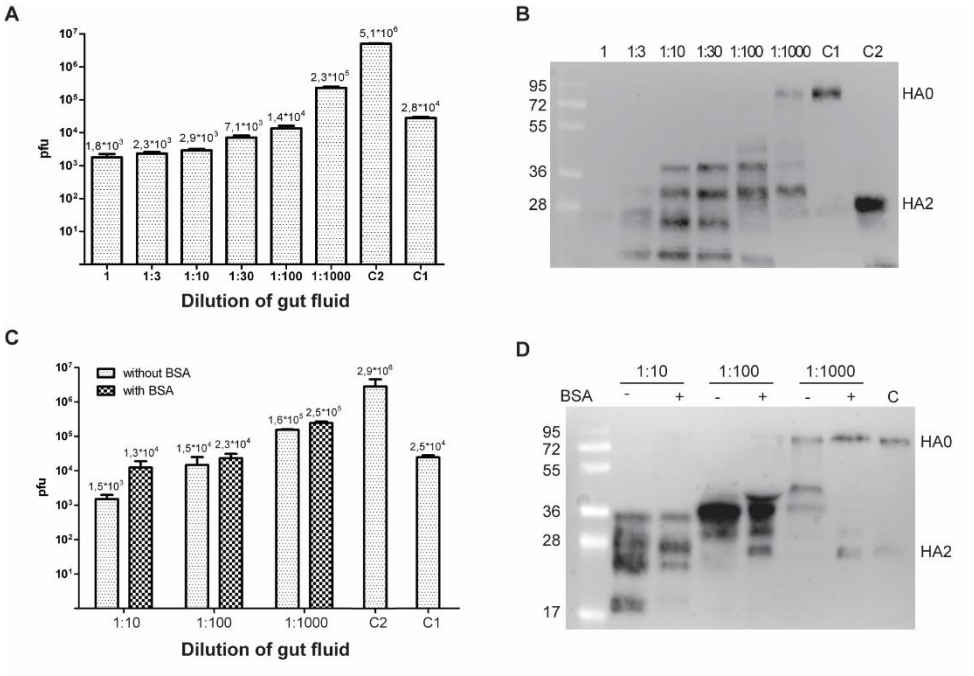

Fig.5.5: Incubation of FPV with intestinal fluid

(A) FPV M1 (10 µl) was incubated for 20 minutes with 60 µl intestinal fluid serially diluted with buffer adjusted to pH 6.5. Viral titers were determined with a plaque assay. C1: 10 µl virus not treated with trypsin. C2: 10 µl of the virus preparation activated with trypsin. The mean of three different incubations including standard deviation is shown.

(B) Aliquots of the samples from A were subjected to SDS-PAGE and western blot using antisera against the HA2 subunit. Controls: virus particles with uncleaved (C1) and cleaved HA (C2) as size marker for the SDS-PAGE mobility of HA0 and HA2, respectively. Numbers indicate the size (kDa) of molecular weight markers.

(C) FPV M1 was incubated with serial dilutions of gut fluid for 20 min without (-) or with (+) additional BSA (1 µg/µl). Viral titers were determined with a plaque assay. C1: 10 µl virus not treated with trypsin. C2: 10 µl of the virus preparation activated with trypsin. The mean of three different incubations including standard deviation is shown.

(D) Aliquots of samples from C were then subjected to SDS-PAGE and western blot using antisera against the HA2 subunit. Virus particles with partially cleaved HA as size marker.

Then this experiment was performed with the low-pathogenic avian virus that was isolated from cloacal swabs of a duck. Plaque assays revealed that this virus is already activated at the low dilution of 1:10; at a dilution of 1:100 and 1:1000 (almost) to the same extent as trypsin treatment (Fig. 5.6). However, undiluted gut fluid and gut fluid diluted 1:3 reduced virus titers, but some infectivity persists.

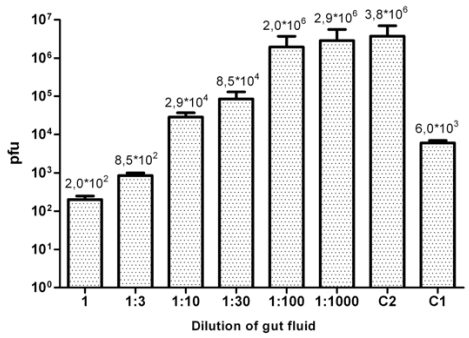

Fig.5.6: Incubation of A/duck/77 with intestinal fluid

A/duck/77 was incubated with serial dilutions of gut fluid for 20 min. Samples were then subjected to plaque assay. C1: 10 µl of the preparation not treated with trypsin. C2: 10 µl virus activated with trypsin. The mean of three different incubations including standard deviation is shown for all plaque assays.

In sum, only highly diluted gut fluid (1:1000) is able to activate FPV with an uncleaved HA. At lower dilutions virus particles are inactivated which is due to degradation of HA (and probably other viral proteins). The duck virus is apparently better adapted to grow in the intestine of birds compared to FPV M1 since it is activated at lower dilutions of gut fluid.

5.2 Characterization of new chicken intestinal epithelial cell lines

5.2.1 Cell morphology and growth

Witek et al. established enterocyte cell lines from specific pathogen-free white Leghorn chicken eggs. Briefly, primary cells were isolated from the intestine of 18-day old embryos and then immortalized by overexpression of hTERT and tumor suppressor gene p53. I received six clones, called 8E11, 9E6, 2GU, T12, T7 and T3. All of these clones propagate healthily in tissue culture flasks and no signs of senescence were noticed, even after multiple passages. Observed in the microscope, the clones show a compact epithelial morphology. Clone 8E11 and T7 are characterized by smaller and spindle-like shaped cells, while larger and prolonged cells can be recognized for cell clone 9E6, T3, T7 and T12 (Fig.5.7A).

I noticed that the time point and cell numbers of seeding of the chicken cells are critical for subculture. The cell-cell contact seems to be critical for recovery, thus a higher concentration of cells from the parental population is preferred during the culture process. Another important point is the temperature. Cold culture medium or standing for long times at room temperature harm the health of cells. Growth curves were determined for clone 8E11 (passage 83) and T12 (passage 29) (Fig.5.7B). The same numbers of cells ($1.5x10^5$) were seeded into one well of 12-well-plate and cell numbers were measured every 12 hours. During the first 24 hours, cells showed similar growth behavior and from then on 8E11 proliferated more rapidly in comparison to T12. 8E11 grew to confluency at 72 hours, whereas T12 achieved confluency at 108 hours post seeding, but with a slightly smaller number of cells than 8E11. The doubling time of clone 8E11 and T12 were determined to be 24.13 hours and 39.73 hours, respectively.

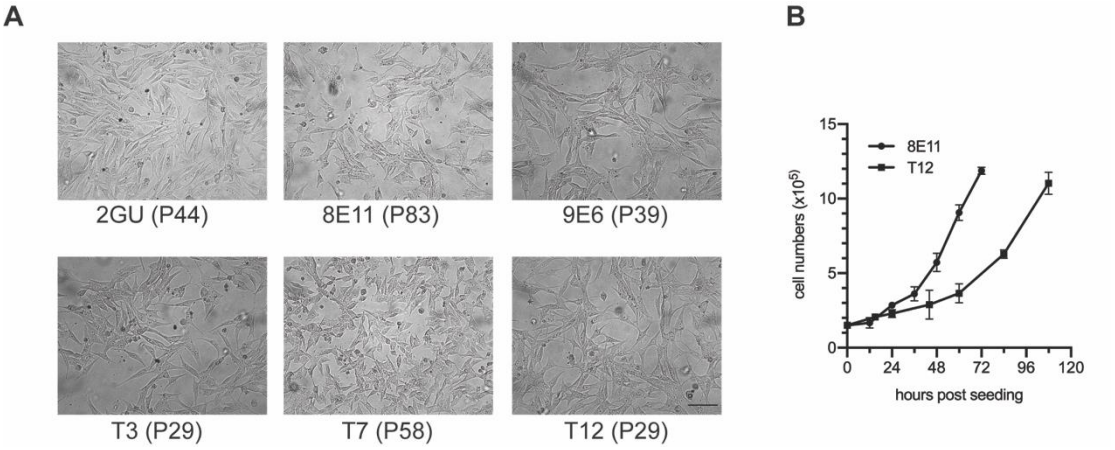

Fig.5.7 Morphology and growth curve of chicken intestinal epithelial cell clones.

(A) The indicated cell clones were seeded in culture dishes. Cells grow as adherent cultures. Pictures were taken with 20X objective by Axiovert A1 Zeiss microscope. Bar 100 µm.

(B) Growth curve of clone 8E11 and T12. $1.5x10^5$ cells were seeded in a well of 12-well-plates and 3 wells of cells were counted every 12 hours with CASY® cell counter. The graph shows the mean cell number including standard deviation from three wells.

5.2.2 HA cleavage in 8E11 cell

To estimate the susceptibility of the chicken intestinal cells to Influenza viruses, the 8E11 cells were infected at a low moi (0.00005) with FPV M1 and WSN/33, respectively in the absence of trypsin and HA- and plaque-titers were determined (Fig. 5.8). Only in the presence of trypsin hemagglutinating and infectious virus were detected in the supernatant. The dependence on trypsin suggests that 8E11 cells are not able to properly process HA with monobasic cleavage site.

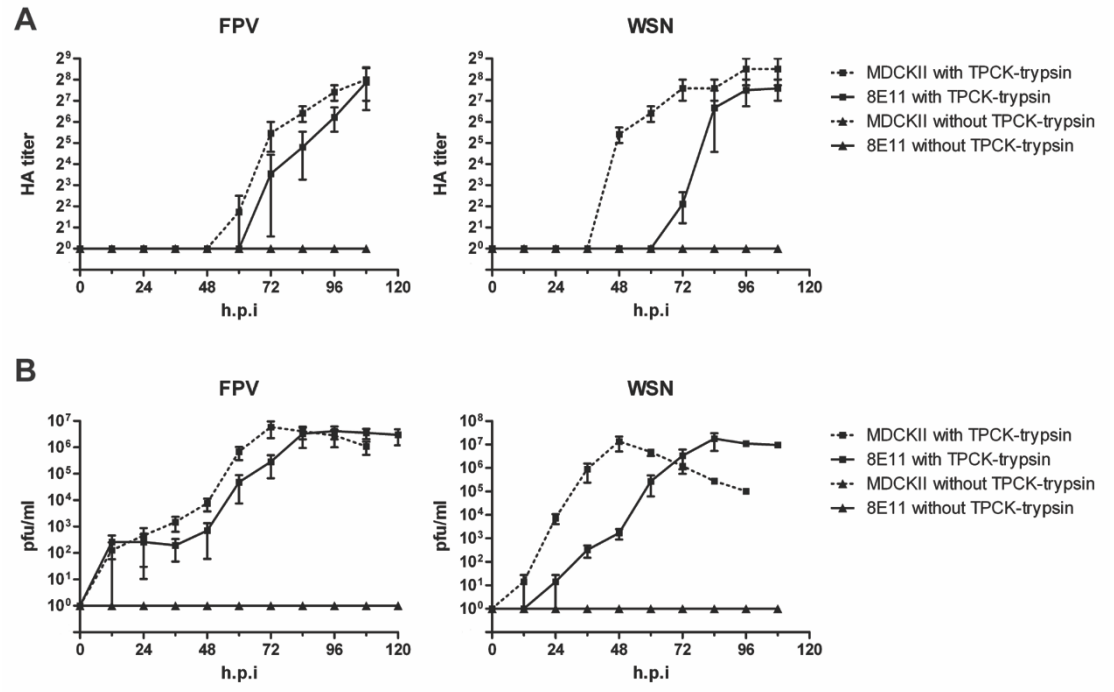

Fig. 5.8: Avian FPV M1 and human WSN virus grow to high titers in the chicken epithelial gut cell line 8E11, but only in the presence of trypsin

8E11 and MDCK II cells were infected with avian FPV M1 or human WSN virus at an MOI of 0.00005 and incubated in the absence or presence of trypsin. At the indicated time points aliquots of the supernatant were removed and HA- **(A)** and plaque-titers **(B)** were determined. Results are shown as the mean including standard deviation of three experiments.

To confirm this, I infected 8E11 cells with FPV-M1 at a moi of 1 with or without trypsin and analyzed cell lysates by Western-blotting with HA2 specific antiserum. With exogenous trypsin HA is almost completely cleaved into the HA2 subunit, whereas in its absence HA remains predominantly uncleaved (Fig. 5.9A). The small amount of a HA2 band that runs below the major HA2 band generated by trypsin is probably functional, since virus grown in the absence of trypsin exhibit low infectivity (titer), which is activated 200 fold by trypsin treatment (titer). Similar result was obtained if T12, T3 and T7 cells were infected (Fig. 5.9B). Thus, similar to most other cell lines, the chicken intestinal cells do not express a protease that completely activates Influenza viruses having an HA with monobasic cleavage site.

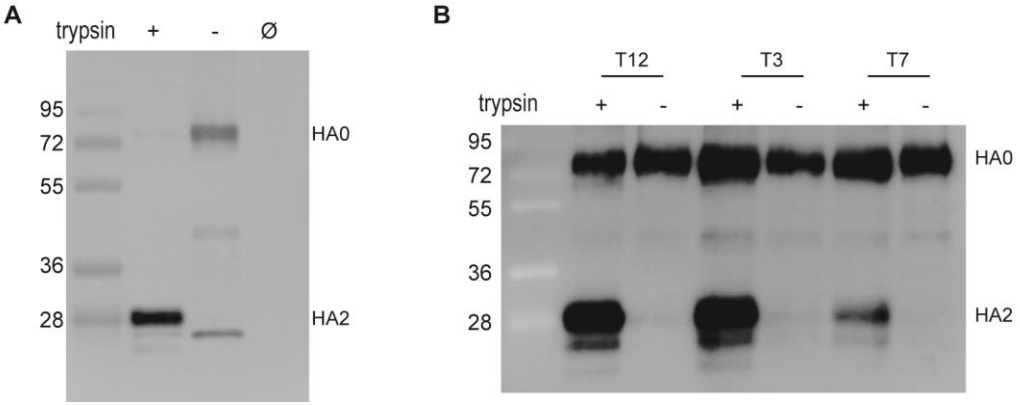

Fig.5.9: Chicken intestinal cells do not cleave HA with monobasic cleavage site

8E11**(A)**, T12, T3 and T7 cells **(B)** were infected at an MOI of 1 with FPV M1 containing HA with a monobasic cleavage site and incubated in the absence (-) or presence (+) of trypsin (2 µg/ml) for 12 hours. Cell lysates were subjected to SDS-PAGE and western blot using antisera against the HA2 subunit.

To investigate whether 8E11 cells process HA with a polybasic cleavage site, HA from the authentic FPV strain (cleavage site PSKKRKKR) and from the mutant 1 (cleavage site PSKGR) were cloned into the expression vector pCAGGS, followed by transfection of 8E11 and HA analysis by western-blotting. As expected, HA with a monobasic cleavage site also remains almost completely uncleaved, whereas HA with polybasic site is properly processed in transfected 8E11 cells (Fig. 5.10A).

HA of HPAIV is usually cleaved by the ubiquitous transmembrane protease furin, which is located in the trans-Golgi network and at the cell surface and cleaves HA during its intracellular transport (85, 151). To investigate whether furin is also responsible in 8E11 cells for cleavage of HA with polybasic cleavage site, we used the peptidomimetic furin inhibitor MI-701, which blocks processing of H5 and H7 subtype HAs and replication of the corresponding viruses in MDCK cells (87). Presence of the drug in 8E11 cells transfected with polybasic HA clearly

inhibits processing at concentrations between 25 µM and 150 µM (Fig. 5.10B), which are only slightly higher than reported for MDCK cells (87).

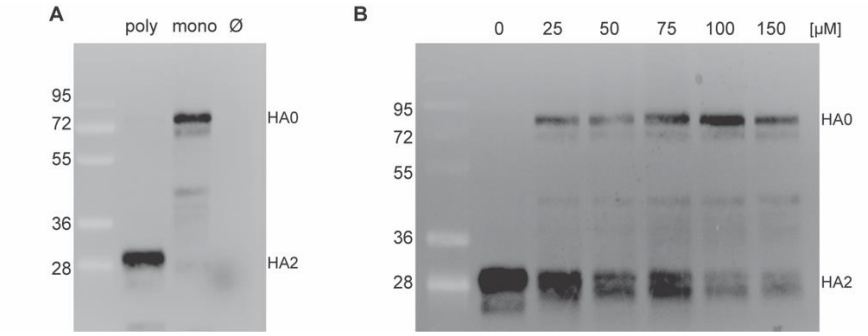

Fig.5.10: 8E11 cells cleave HA with polybasic, but not with monobasic cleavage site

(A) HA from FPV containing a monobasic (mono) or a polybasic (poly) cleavage site was expressed in 8E11 cells. Cell lysates were then subjected to western blot using antiserum against the HA2 subunit. Ø: uninfected or untransfected cells.

(B) HA from FPV containing a polybasic cleavage site was expressed in 8E11 cells. 1 h after transfection the furin inhibitor MI-701 was added to the indicated final concentrations (µM).

In sum, the chicken gut epithelial cell line 8E11 supports replication of avian and human Influenza viruses to high titers, cleaves HA from HPAIV with furin, but contains no enzyme for efficient processing of HA from low pathogenic avian Influenza viruses which are thus released mainly in a non-infectious form.

5.2.3 Replication of human Influenza viruses in 8E11 and T12 cells

Furthermore, cell susceptibility to Influenza viruses in the presence of exogenous trypsin were tested with three more Influenza A strains, one Influenza B strain and one Influenza C strain. Growth kinetics of viruses in 8E11 and T12 were compared with the standard cell line MDCK. Results are shown in Table 5.1.

For avian Influenza strain FPV M1 a moi of 0.00005 was used for infection. Viruses grow to high titers ($4.11x10^6$ pfu/ml) in 8E11, very similar as in MDCKII cells, but viral replication kinetics are slower. In T12 cells virus grow slower and to lower titers ($6.3x10^5$ pfu/ml) compared to MDCK II cells. The other tested avian strain duck/77 grows to higher titer in MDCKII than in 8E11 and T12, i.e. $1.36x10^5$ pfu/ml compared to $7.26x10^4$ pfu/ml and 9.14 $x10^3$ pfu/ml. The human Influenza strains, WSN/33 (H1N1, moi 0.00005) and Panama/99 (H3N2, moi 0.0005) show similar growth patterns as avian strains, viruses replicate productively in 8E11, but to a lower titer in T12. However, a more recent H1N1 strain New Caledonia/99 does not propagate as efficiently as in MDCKII.

Growth of Influenza B virus on the two clones of intestinal cells were also compared to MDCK cells. B/Lee/40 was used to infect at a moi 0.005. Virus titers peak at 4 and 6 d.p.i in T12 and 8E11 (~$5x10^5$ pfu/ml), which was lower than titers in MDCK cell at 3 d.p.i. In contrast, Influenza C virus strain C/JJ/50 demonstrated faster growth and higher HA titers in chicken intestinal cell lines than in MDCKI cells.

Table5.1 Virus replication in 8E11 and T12

Virus strain	moi	Cell type	Peak virus titer		Time point when reach peak pfu/HAU
			pfu/ml	HAU	
A/FPV/Rostock/34 (H7N1) M1	0.00005	MDCKII	5.91 x10^6	2^7	72 h.p.i
		8E11	4.11x10^6	2^7	96 h.p.i
		T12	6.30x10^5	2^6	108 h.p.i
A/duck/Bavaria/1/77 (H1N1)	0.001	MDCKII	1.36 x10^5	2^9	36 h.p.i
		8E11	7.26x10^4	2^9	48 h.p.i
		T12	9.14x10^3	2^8	60 h.ip.i
A/WSN/33 (H1N1)	0.00005	MDCKII	1.33x10^7	2^7	48 h.p.i
		8E11	1.76x10^7	2^7	84 h.p.i
		T12	2.47x10^6	2^6	96 h.p.i
A/Panama/07/99 (H3N2)	0.0005	MDCKII	6.05x10^7	0	72 h.p.i
		8E11	6.21x10^6	0	96 h.p.i
		T12	3.56x10^4	0	120 h.p.i
A/New Caledonia/00/99 (H1N1)	0.0005	MDCKII	3.02x10^6	0	60 h.p.i
		8E11	4.63x10^3	0	108 h.p.i
		T12	8.21x10^3	0	120 h.p.i
B/Lee/40	0.005	MDCKI	2.00x10^6	2^4	3 d.p.i
		8E11	3.20x10^5	2^7	6 d.p.i
		T12	6.20x10^5	2^6	4 d.p.i
C/JJ/50 (NS of C/JHG/66)	0.05	MDCKI	n. d.*	2^4	6 d.p.i
		8E11	n. d. *	2^7	6 d.p.i
		T12	n. d. *	2^6	5 d.p.i

* Plaque assay were not performed with Influenza C virus

5.2.4 Replication of Newcastle disease virus in 8E11 and T12 cells

Furthermore, I tested susceptibility of cells to Newcastle disease virus, which is also an important viral pathogen in avian species. Growth behavior of velogenic NDV Italien strain was tested in 8E11 and T12 cells, using CEF as comparison. Cells were infected at a moi of 0.00005 and virus propagated rapidly in all tested cells. The highest infectious titer is 10^7 pfu/ml at 36 h.p.i in both 8E11 and T12, while CEF achieved a slightly lower titer (6x10^6 pfu/ml).

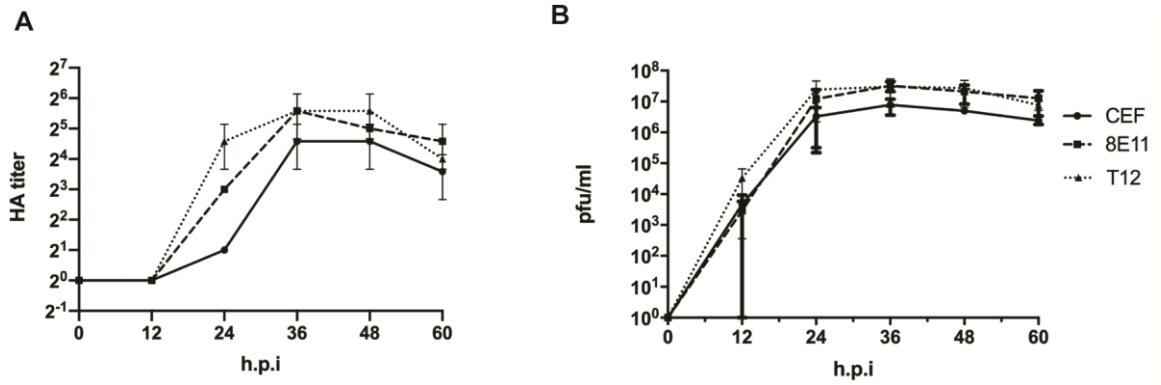

Fig.5.11 Newcastle disease virus italien strain grow to high titer in the CHIC 8E11 and T12 in the absence of trypsin.

8E11, T12 and CEF cells were infected with NDV italien at an MOI of 0.00005 and incubated in the absence of trypsin. At the indicated time points aliquots of the supernatant were removed and HA-**(A)** and plaque-**(B)** titers were determined. Results are shown as the mean including standard deviation of two experiments.

5.2.5 Plaque formation in 8E11 cells

Plaque assay is commonly used for virus titration. Since the previous data indicate that all the tested Influenza strains (except New Caledonia) and NDV propagate productively in intestine 8E11 cell, I asked whether the cell can be used for plaque titration of viruses. FPV M1, NDV italien strain were diluted and proceeded to standard plaque titration in monolayers of 8E11 using MDCKII or CEF in comparisons. At 2 d.p.i, the plaque diameter of FPV M1 in 8E11 is about half of that in MDCKII, while at 3 d.p.i the plaque size enlarged to a similar size of that in MDCKII (2 d.p.i). This agrees with our growth kinetic, i.e. that viruses grow slower in 8E11 cell. On the contrary, NDV Italien forms approximately twice the diameter of plaques in 8E11 than those observed in CEF (Fig.5.12).

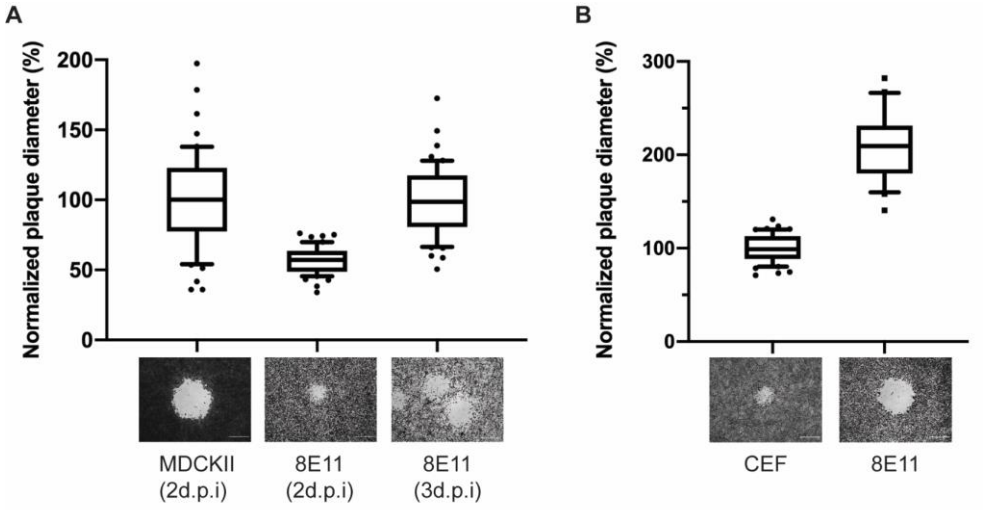

Fig.5.12 Avian FPV M1 and NDV italien form plaques in the CHIC 8E11 when incubated with overlay medium.

8E11 were infected with avian FPV M1**(A)** and NDV italien strain **(B)** of known titer and covered with overlay medium. MDCKII or CEF were used for comparison. The average plaque diameters from three independent experiments are shown in a box plot (normalized to that of MDCK II or CEF cells). The whiskers cover 10%-90% of the data with 10% smallest and largest plaques shown with dots. Representative images of plaques are shown below (Bars 1 mm).

5.2.6 Transfection and application of 8E11 in reverse genetics

Reverse genetics systems allow the production of Influenza viruses from cloned viral cDNA. In this study, I first explored whether 8E11 can be easily transfected using a standard plasmid that expresses GFP. Approximately 30% of 8E11 expressed a fluorescent signal when pCGFP plasmid was transfected, which is only slightly lower compared to transfected 293T cell (Fig.5.13A).

Then I tried to rescue FPV M1 with a 12-plasmids system as described before. After transfection of 8E11, 293T or a co-culture of 8E11/293T cells, the supernatants were collected and incubated with MDCK cells to get a passage 1 (P1) virus. The resulting supernatants from the 8E11-transfection showed neither HA- nor plaque titer. In contrast, P1 from the 293T-transfection showed an HA titer of 2^3 and a plaque titer of $1.25x10^5$ pfu/ml. The P1 supernatant from co-culture transfection achieved an HA titer of 2^6 and a plaque titer of $1.48x10^5$ pfu/ml (Fig.5.13B). Thus, 8E11 cells are transfectable, but could only produce Influenza viruses when co-cultured with 293T cells.

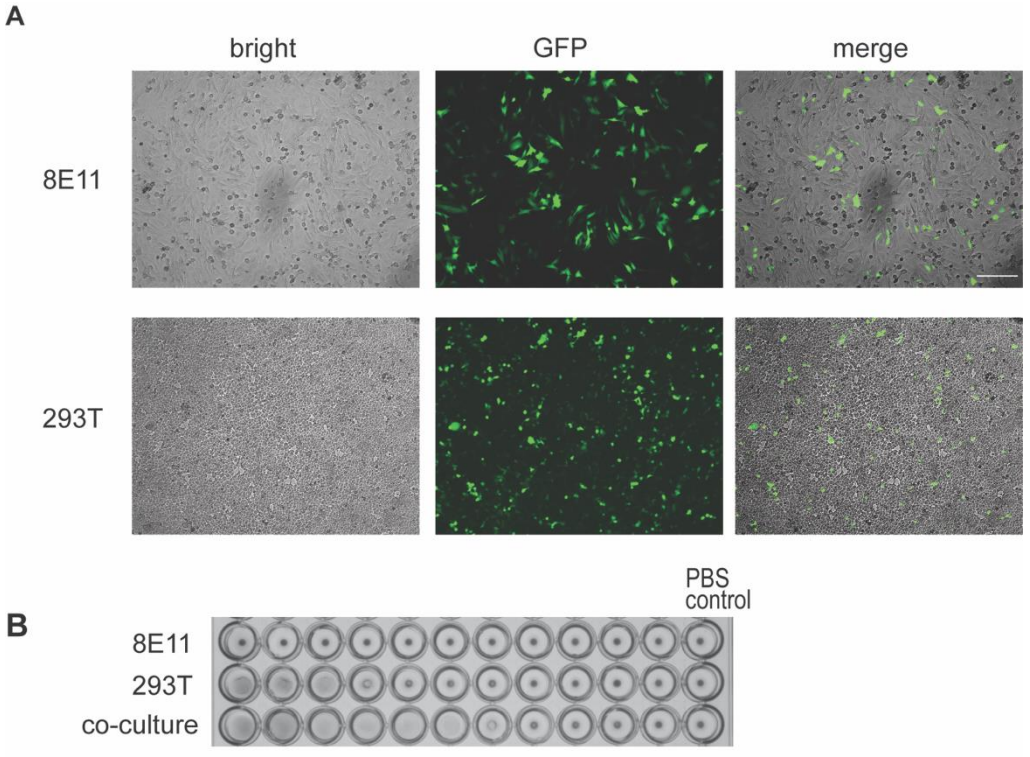

Fig.5.13 Transfection efficiency of 8E11 and rescue of FPV M1 virus from 293T/8E11 co-culture system.

(A) 8E11 and 293T express GFP at 3 days post pEGFP plasmid transfection. Pictures were taken with 10X objective by Axiovert A1 Zeiss microscope. Bars 200 µm.

(B) Rescue of FPV M1 was confirmed by HA test of P1 supernatant.

5.2.7 Polarization of 8E11 cell

In vivo, the intestinal epithelial cells form a barrier between the intestinal lumen and the organism's interior by formation of tight and adherens junctions between individual enterocytes and maintenance of such cellular polarity. Here I asked whether 8E11 cell polarize in vitro using the adherens junction protein β-Catenin as a marker. However, fluorescence microscopy showed that the protein was expressed all over the cell membrane 3 or 5 days after seeding. At 7 days after seeding, multilayers of cells were observed with β-Catenin expressed in and between cell membranes. As a control for successful polarization, MDCKII were grown under the same conditions. At 5 or 7 days post seeding, β-Catenin was detected in the basolateral part of the cell membrane, but not in the apical part, which indicated formation of adherens junctions between cells and hence cell polarization.

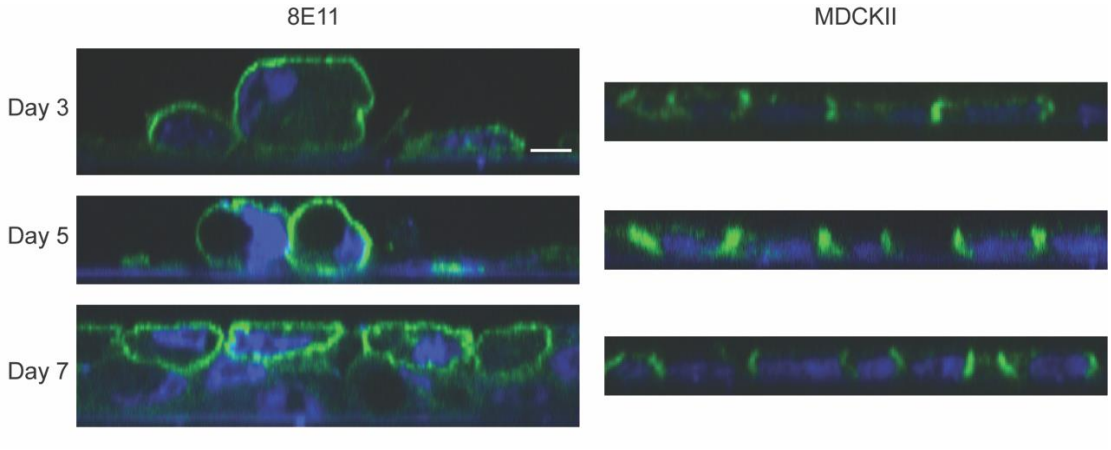

Fig.5.14 8E11 cells do not polarize under tested conditions.

8E11 cells were seeded onto 12mm transwell filters coated with 1.5µg/ml collagen solution. 3, 5, 7 days after seeding, the membrane filter with cells were cut off from the transwell and cells were fixed. Adherens junction protein β-Catenin was detected by mouse anti-β-Catenin (1:500) as primary antibody, followed by secondary goat anti-mouse IgG-Alexa 488. Cell nuclei were stained with DAPI (1:5000). Z-stacks with 0.5 µm increments of cells were combined and shown. Bar 5 µm. β-Catenin was expressed all over the surface of 8E11 cells but only in the basolateral part of MDCK II.

6 Discussion

6.1 Mimicking the passage of avian Influenza viruses through the gastrointestinal tract of chickens

I analyzed whether two avian Influenza viruses might survive the passage through the gastrointestinal tract of birds by incubating virus particles with fluids obtained from the gizzard and the first part of the intestine of chickens. Gizzard fluid completely inactivates $5x10^6$ infectious particles of a mutant of fowl plague virus (FPV) harboring a HA with a monobasic cleavage site, even if the gizzard fluid is highly diluted at acidic pH. The same was observed for a virus originally isolated from cloacal swabs of a duck. This is due to the low pH of the gizzard (pH 3.5), since at pH 4 the same amount of virus is also (almost) completely inactivated. In addition, HA (and probably other viral proteins) are most likely degraded by the protease pepsin even if samples were supplemented with additional protein (Fig. 5.1)

These inactivation experiments are compatible with recent studies about survival of two human enveloped viruses in juices from the gastrointestinal tract. Hantavirus (titer $5x10^5$) is completely inactivated after incubation for 15 minutes with human gastric juice adjusted to pH 1 or pH 3. Juice adjusted to pH 4 or pH 5 inactivated 99% and 90%, respectively of infectious particles (152). Likewise, MERS-coronavirus (titer $7.5x10^6$) is completely inactivated after an incubation for 30 minutes in fasted state simulated gastric fluid (pH 1.6, containing pepsin), but stable in a solution simulating the gastric fluid after food uptake (pH 5, but no pepsin) (153). Taken together, enveloped viruses are apparently rapidly and quantitatively inactivated at a pH below 5. In contrast, non-enveloped viruses known to be transmitted by the fecal-oral route, such as rotaviruses are completely stable at pH 4, partly and slowly inactivated at pH 3 and only at pH 2 rapidly and completely lose their infectivity (154).

I only had access to gastrointestinal fluids from chickens, but the natural host and the reservoir of avian Influenza viruses are water birds and one might argue that less acidic conditions might prevail in their stomachs. However, a recent investigation points out that chickens possess the highest pH in the stomach of all Aves (~3.5). The pH of the gizzard in water birds susceptible to Influenza infection is more acidic; pH 2.2 in the mallard duck (*Anseriformes*), 1.5 in black headed gull and 1.2 in common pied oystercatchers (*Charadriiformes*) (139, 155).

However, if the gizzard fluid is diluted with neutral buffer, a different picture emerges (Fig.5.2, Fig.5.3). Even at a low dilution of 1:10 viruses having an uncleaved HA are activated almost to the same extent as cleavage with trypsin. Thus, it is tempting to speculate that if water contaminated with viruses is swallowed by a water bird, it might neutralize the otherwise destructive acidic pH of the gizzard and therefore virus particles are neither denatured nor digested by the acidic protease pepsin. Even more, a trypsin-like protease present in the gizzard fluid now becomes active that cleaves HA at the proper site and thus activates virus particles. More research is required to characterize this proteolytic activity further.

In principle, cleavage of HA with monobasic cleavage site can be achieved by the digestive enzyme trypsin present in the gut fluid. Trypsin activates virus particles with uncleaved HA even at concentrations 100-fold higher (2000 µg/ml) than usually used in multiple cycle growth experiments, although some degradation of the HA2 band is observed under those conditions (Fig.5.4). Indeed, viruses are activated by the gut fluid, but a remarkable difference exists between the viruses isolated from a chicken (FPV) and from cloacal swabs of a duck (A/duck/77). Both are slightly inactivated by undiluted gut fluid, but the duck virus is already

activated at a dilution of 1:10, whereas FPV M1 requires a dilution of 1:1000 for the same effect (Fig.5.5, Fig.5.6). Thus, the duck virus is apparently better adapted to grow in the intestine of birds compared to FPV M1.

6.2 Characterization of a new chicken intestinal epithelial cell line

Avian Influenza viruses were reported to not only replicate in the avian respiratory tract, but also in the intestinal tract and were detected in feces during natural or experimental infection of birds. To date, MDCK cells (i. e. cells from the kidney of dogs, which are not a natural target of Influenza infection in vivo) serve as the major in vitro cell model for Influenza studies, but many groups attempted to establish primary or immortalized cells from different hosts to better study host-pathogen interaction in more relevant cell lines. The first chicken intestinal epithelial cell lines were generated and made available to us by the company “MicroMol”. To test whether these cell lines represent a suitable in vitro model for evaluation of Influenza virus infection in chicken cells of the digestive system was another aim of my study. The main questions I wanted to address were: 1) Can these cell lines be stably passaged in vitro? 2) Do these cells support infection with Influenza viruses and Newcastle disease virus and produce infectious virus particles comparable to that in MDCK or CEF cells? 3) Do these cells contain proteases that process HA with monobasic and polybasic cleavage site? 4) Is it possible with the cell lines to rescue Influenza virus with reverse genetic system?

Primary cells minimize the genotypic and phenotypic variations usually associated with immortalized cell lines and thus better mimic the donor tissue. However, due to difficulties in obtaining primary cells and their limited life span, immortalized cell lines that retain constant characteristics following numerous passages become an alternative cell system. The chicken epithelial cell lines used in the study were immortalized from primary culture by overexpression of hTERT and tumor suppressor gene p53. All the clones tested show a polygonal or spindle-like morphology. Clone 8E11 and T12 were used for further study. Their physical condition retains over passage 90 (or even more) with a shorter doubling time of 8E11 than T12.

Epithelial cells in the respiratory and intestinal tract were suggested to be permissive to Influenza viruses and Newcastle Disease viruses based on in vivo studies (156,157). The chicken lung epithelium cell line (CLEC213) has been shown to be permissive to four different LPAI subtypes, but produced less infectious particles, when compared with MDCK cells (73). A primary chicken intestine epithelial cell (IEC) was established by Kaiser and colleagues and was shown to be susceptible to LPAIV A/chicken/Saudi Arabia/CP7/1998 (H9N2) and velogenic viscerotropic NDV (vvNDV) Herts 33/56. H9N2 achieved more than 1000-fold higher titer in IEC than in CEF, while vvNDV Herts 33/56 propagated similarily in both cells (64). Susceptibility to human Influenza strains or Influenza B or C were not tested in either CLEC213 or IEC.

In this study, chicken intestinal epithelial cell clones 8E11 and T12 were shown to be permissive to two LPAIVs, three human Influenza strains, one Influenza B and one recombinant Influenza C in the presence of exogenous trypsin, as well as vvNDV italien in the absence of trypsin. A/FPV/Rostock/1934-M1 (avian H7N1) and A/WSN/33 (human H1N1) achieved a similar titer in 8E11 cells at later time points compared to MDCKII, while A/duck/Bavaria/1977 (avian H1N1), A/Panama/2007/1999 (human H3N2) and A/New Caledonia/2000/1999 (human H1N1) reached a lower titer. vvNDV italien formed clear plauqes and grew rapidly in both chicken intestinal cell lines, achieving higher titers compared to primary chicken embryo fibroblasts

(CEF). The vvNDV propagate in 8E11 or T12 faster than any tested Influenza strain, even at a very low moi (0.00005). This might indicate a higher tropism of NDV to the chicken intestine.

The more recent human H1N1 strain A/New Caledonia/20/1999 is a seasonal vaccine strain used during the 2000/01–2006/07 Influenza seasons. It does not grow to the same high titers in the chicken intestinal cells compared to the other tested human H1N1 strain A/WSN/33, although I tested many different conditions (moi, TPCK-trypsin concentration). I also observed that it does not hemmaglutinate chicken red blood cell, even if the infectious titer reached more than 10^6 PFU/ml (Table 5.1). One possible reason for the differences is the alteration in glycosylation of HA during viral antigenic drift over time, which could influence a wide range of biological features of the virus. Eight N-glycosylation sites were identified in the HA of A/New Caledonia/20/1999, four of them are absent in the HA of A/WSN/1933 (156,159). The newly acquired glycosylation sites N142 and N177 of A/New Caledonia/20/1999 are located in the vicinity of the receptor binding site, and thus they might alter the host receptor affinity of this strain (159).

Another important feature is the receptor expression in the cell surface, which is the basic determinant of Influenza tropism. HA of Influenza A and B viruses binds multivalently to non-O-acetylated N-acetylneuraminic acid. Human Influenza virus HAs preferentially bind to cell surface receptors with α2,6-linked sialic acid, whereas avian Influenza HAs preferentially bind to receptors with α2,3-linked sialic acid. In this study, three human Influenza strains as well as two avian strains were shown to infect 8E11 and T12 indicating that the cell lines contain both types of receptors. This is in accordance with the results of experimental studies where it was shown that both α2-3 and α2-6 sialic acid receptors are expressed in the intestinal tract of chickens (119,120). Furthermore, since Influenza C virus also infects 8E11 cells, the cells must express also the N-acetyl-9-O-acetylneuraminic acid receptor which this virus uses to infect cells.

Nevertheless, only α2-3 sialic acid receptor exists in intestinal tract of mallard (duck), which correlates with the fact that ducks are resistant to the infection with human Influenza A viruses (160). Assuming that the properties of the 8E11 and T12 cell lines faithfully reflect native cells in the chicken's intestine, the chicken intestinal epithelium could be susceptible to both avian and human strains, which indicates the role of chicken as potential intermediate host for Influenza transmission between avian and human.

Influenza HA with a multibasic consensus motif can be cleaved by an ubiquitous protease, while HAs with monobasic cleavage site require exogenous trypsin in vitro. In my study, FPV M1 and WSN having a HA with a monobasic cleavage site require trypsin for growth under multiple cycle conditions (moi 0.00005) and monobasic HA also remained almost completely uncleaved in transfected chicken 8E11 cells. Thus, 8E11 cells do not express a cellular protease that can fully cleave HA with monobasic cleavage site. This is somewhat in contrast to infection experiments with a primary intestine epithelial cell IEC. Kaiser et al. claimed that the LPAIV H9N2 reached a virus titer of about 10^7 FFU/ml (Focus Forming Units/ml) when IECs were infected at an moi of 0.01 in the absence of exogenous trypsin. However, they also reported that only less than 30% of cells were infected after 24 h. p.i (64), indicating that the virus was not fully activated by cellular protease. In my study I found that 8E11 process HA with polybasic cleavage site, probably by the ubiquitous enzyme furin. The results also indicate that only highly pathogenic Influenza viruses are released by chicken gut cells as infectious

particles while low pathogenic Influenza viruses require an exogenous protease for cleavage of HA.

Furthermore, the chicken intestinal epithelial cells can be used as an alternative cell line in a reverse genetics system. 8E11 can be efficiently transfected, but apparently do not produce infectious Influenza viruses with the plasmid system I tested. A possible reason might be that the human RNA polymerase I promotor does work only in mammalian cells and hence the viral genome cannot be transcribed in avian cells. However, if the 8E11 cells are co-cultured with human 293T cells, infectious virus particles are recovered, probably because 293T cells produce infectious virus particles after transfection which are then amplified in 8E11 cells. Zhang's group constructed a one-plasmid system having all Influenza virus genome on a single plasmid with a CMV promotor, which is supposed to work in all eukaryotic cell lines (38). I would assume that this system is also applicable in 8E11 cell, enabling a simpler approach.

In sum, the tested chicken intestinal epithelial cell lines would serve as a good in vitro model for studying pathogen-host interactions at the mucosal interface of the chicken intestinal tract.

Zusammenfassung

Nachahmung der Passage des Vogelgrippevirus durch den Magen-Darm-Trakt von Hühnern und Charakterisierung neuartiger Hühner-Darm-Epithelzelllinien

Das Influenzavirus ist ein ansteckender Erreger mehrerer Wirte, einschließlich Menschen, anderer Säugetiere und Vogelarten. Bei Menschen und anderen Säugetieren infizieren Viren normalerweise das respiratorische Epithel und werden über die Luft übertragen.

Im Gegensatz dazu infiziert es bei Vögeln auch den Intestinaltrakt und überträgt sich hauptsächlich über den fäkal-oralen Weg. Das Glykoprotein Hämagglutinin (HA) des Influenza-Virus spielt eine entscheidende Rolle bei der Rezeptorbindung und der anschließenden Fusion des Virus mit einer Wirtsmembran. Die proteolytische Prozessierung von HA in die HA1- und HA2-Untereinheiten durch Trypsin-ähnliche Proteasen und eine irreversible Konformationsänderung, induziert durch den sauren pH-Wert, sind für die Membranfusion erforderlich. Ein saurer pH-Wert (wie er im Muskelmagen von Vögeln vorherrscht) inaktiviert jedoch Viruspartikel und eine hohe Konzentration an Trypsin sowie anderen Verdauungsproteasen, wie Pepsin und Chymotrypsin, verdaut HA proteolytisch.

In dieser Studie ahmte ich die Passage von Viren durch den Magen-Darm-Trakt nach, indem ich zwei Vogelgrippestämme mit Muskelmagen- und Darmflüssigkeit von Hühnern inkubierte und die Virustiter und die Integrität von HA mittels Western-Blot bestimmte. Die Muskelmagenflüssigkeit inaktivierte Viren vollständig und degradierte HA selbst bei einer hohen Verdünnung, jedoch nur, wenn der pH-Wert sauer gehalten wurde. Wenn die Flüssigkeit mit neutralem Puffer verdünnt wird (was die die Virusaufnahme mit Seewasser imitiert), sind die Partikel widerstandsfähiger. Viren, die ungespaltenes HA enthielten, wurden sogar aktiviert, was darauf hindeutet, dass Magensaft eine Trypsin-ähnliche Protease enthält. Unverdünnte Darmflüssigkeit inaktivierte Viruspartikel und zerstörte HA, aber verdünnte Flüssigkeit aktivierte diese Viren. Somit können Influenzaviren unter bestimmten Bedingungen den zerstörerischen Flüssigkeiten des aviären Verdauungstrakts widerstehen.

In dieser Hinsicht besteht ein bemerkenswerter Unterschied zwischen einer Mutante des Geflügelpestvirus (FPV M1) und einem aus Entendarm isolierten Virus (A/duck/Bavaria/77). Während FPV M1 eine hohe Verdünnung von 1: 1000 erfordert, um aktiviert zu werden, inaktivieren niedrigere Verdünnungen das Virus und degradieren HA. Im Gegensatz dazu wird das von Enten stammende Virus bereits bei einer Verdünnung von 1:10 aktiviert. Daher ist das Entenvirus gegenüber Darmflüssigkeit toleranter als das Geflügelpestvirus, was darauf hindeutet, dass ersteres besser für das Wachstum im Darm von Vögeln geeignet ist.

Bisher waren keine Zelllinien aus dem Darm von Vögeln verfügbar. Hier habe ich eine neue Hühnerdarmepithelzelllinie getestet, die wir von der Firma „MicroMol“ bezogen haben. Die Zelllinien besitzen eine typisch epitheliale Morphologie und zeigen bei wiederholter Passage keine Anzeichen von Seneszenz. Die Zelllinien sind permissiv für fünf Influenza-A-Viren (zwei aviären Ursprungs und drei humanen Ursprungs), ein Influenza-B-Virus, ein Influenza-C-Virus und einen velogenen Newcastle-Disease-Virus-Stamm. Diese Zellen prozessieren HA mit einer polybasischen Schnittstelle effektiv, wahrscheinlich durch die zelluläre Protease Furin. Im Gegensatz dazu wird in mehrstufigen Wachstumsexperimenten exogenes Trypsin benötigt, was darauf hinweist, dass Viren mit einer monobasischen HA-Schnittstelle nicht aktiviert werden. Somit haben diese Zellen die gleichen Eigenschaften wie jede andere bekannte Zelllinie, die für eine Influenza-Infektion anfällig ist.

Summary

Influenza virus is a contagious pathogen of multiple hosts, including humans, other mammals and avian species. In humans and other mammalian hosts viruses usually infect the respiratory epithelium and are airborne transmitted. In contrast, in birds it also infects the intestinal tract and transmits primarily via the fecal-oral route. The major glycoprotein hemagglutinin (HA) of Influenza virus plays a vital role in receptor binding and subsequent fusion of the viral with a host membrane. Proteolytic processing of HA into HA1 and HA2 subunits by trypsin-like proteases and an irreversible conformational change induced by acidic pH are required for membrane fusion. However, acidic pH (as it prevails in the gizzard of birds) inactivates virus particles and high concentrations of trypsin as well as other digestive proteases, such as pepsin and chymotrypsin proteolytically digest HA.

In this study, I mimicked the passage of viruses through the gastrointestinal tract by incubating two avian Influenza strains with gizzard and gut fluid from chicken and determined virus titers and integrity of HA by western-blot. The gizzard fluid completely inactivated virions and degrades HA even at a high dilution, but only if the pH was kept acidic. If the fluid is diluted with neutral buffer (mimicking virus uptake with seawater) particles were more resistant. Virions containing an uncleaved HA were even activated suggesting that gastric juice contains a trypsin-like protease. Undiluted intestinal fluid inactivated particles and destroyed HA, but diluted fluid activated virions. Thus, under certain conditions Influenza viruses can withstand the destructive fluids of the avian digestive tract.

A remarkable difference exists in this regard between the fowl plaque virus (FPV M1) and a virus isolated from the duck´s intestine (A/duck/Bavaria/77). While FPV M1 requires a high dilution of 1:1000 to be activated, lower dilutions inactivated the virus and degraded HA. In contrast; the duck-derived virus is already activated at a dilution of 1:10. Thus, the duck-derived virus is more tolerant against intestinal fluid compared to fowl plaque virus suggesting that the former is better adapted to grow in the intestine of birds.

Hitherto, no cell lines from the intestine of birds were available. Here I tested a novel chicken intestinal epithelial cell line, which we obtained from the company “MicroMol”. The cell lines show typical epithelial morphology and do not exhibit any sign of senescence during repeated passage. The cell lines are permissive to five Influenza A viruses (two of avian origin and three of human origin), one Influenza B virus, one Influenza C virus and a velogenic Newcastle Disease Virus strain. These cells effectively process HA with a polybasic cleavage site, probably by the cellular protease furin. In contrast, exogenous trypsin is required in multiple step growth experiments, indicating that viruses with a monobasic HA cleavage site are not activated. Thus, these cells have identical properties as any other known cell line that is susceptible to Influenza infection.

.

References

1. **Webster RG, Bean WJ, Gorman OT, Chambers TM, Kawaoka Y.** 1992. Evolution and ecology of Influenza A viruses. Microbiol Rev **56**:152-79.
2. **Su S, Fu X, Li G, Kerlin F, Veit M.** 2017. Novel Influenza D virus: Epidemiology, pathology, evolution and biological characteristics. Virulence **8**:1580-1591.
3. **Iuliano AD, Roguski KM, Chang HH, Muscatello DJ, Palekar R, Tempia S, Cohen C, Gran JM, Schanzer D, Cowling BJ, Wu P, Kyncl J, Ang LW, Park M, Redlberger-Fritz M, Yu H, Espenhain L, Krishnan A, Emukule G, van Asten L, Pereira da Silva S, Aungkulanon S, Buchholz U, Widdowson MA, Bresee JS.** 2018. Estimates of global seasonal Influenza-associated respiratory mortality: a modelling study. Lancet **391**:1285-1300.
4. **Capua I, Alexander D.** 2010. Perspectives on the global threat: the challenge of avian Influenza viruses for the world's veterinary community. Avian Dis **54**:176-8.
5. **Alexander DJ.** 2007. An overview of the epidemiology of avian Influenza. Vaccine **25**:5637-44.
6. **Tong S, Zhu X, Li Y, Shi M, Zhang J, Bourgeois M, Yang H, Chen X, Recuenco S, Gomez J, Chen LM, Johnson A, Tao Y, Dreyfus C, Yu W, McBride R, Carney PJ, Gilbert AT, Chang J, Guo Z, Davis CT, Paulson JC, Stevens J, Rupprecht CE, Holmes EC, Wilson IA, Donis RO.** 2013. New world bats harbor diverse Influenza A viruses. PLoS Pathog **9**:e1003657.
7. **Jennings L, Huang QS, Barr I, Lee PI, Kim WJ, Buchy P, Sanicas M, Mungall BA, Chen J.** 2018. Literature review of the epidemiology of Influenza B disease in 15 countries in the Asia-Pacific region. Influenza Other Respir Viruses **12**:383-411.
8. **Guo YJ, Jin FG, Wang P, Wang M, Zhu JM.** 1983. Isolation of Influenza C virus from pigs and experimental infection of pigs with Influenza C virus. J Gen Virol **64** (Pt 1):177-82.
9. **Matsuzaki Y, Katsushima N, Nagai Y, Shoji M, Itagaki T, Sakamoto M, Kitaoka S, Mizuta K, Nishimura H.** 2006. Clinical features of Influenza C virus infection in children. J Infect Dis **193**:1229-35.
10. **Medina RA, Garcia-Sastre A.** 2011. Influenza A viruses: new research developments. Nat Rev Microbiol **9**:590-603.
11. **Lamb, R.A. and Krug, R.M. 2001.** *Orthomyxoviridae*: The Viruses and Their Replication. *In*: Knipe, D.M., Howley, P.M. and Griffin, D.E., Eds., Fields Virology, 4th Edition, Lippincott Williams & Wilkins, Philadelphia, 1487-1531.
12. **Wang M, Veit M.** 2016. Hemagglutinin-esterase-fusion (HEF) protein of Influenza C virus. Protein Cell **7**:28-45.
13. **Olsen B, Munster VJ, Wallensten A, Waldenstrom J, Osterhaus AD, Fouchier RA.** 2006. Global patterns of Influenza a virus in wild birds. Science **312**:384-8.
14. **Pantin-Jackwood MJ, Swayne DE.** 2009. Pathogenesis and pathobiology of avian Influenza virus infection in birds. Rev Sci Tech **28**:113-36.
15. **World Organisation for Animal Health (OIE)**. 2018. Chapter 3.3.4. Avian Influenza. In Terrestrial Manual 821-841.
16. **Swayne D.E. & Halvorson D.A.** 2008. Influenza. *In*: Diseases of poultry (Y.M. Saif, J.R. Glisson, A.M. Fadly, L.R. McDougald & L. Nolan, eds). 12th Ed. Blackwell, Ames, Iowa, 153-184.
17. **Swayne DE.** 2007. Understanding the complex pathobiology of high pathogenicity avian Influenza viruses in birds. Avian Dis **51**:242-9.
18. **Alexander DJ.** 2007. An overview of the epidemiology of avian Influenza. Vaccine **25**:5637-44.
19. **Swayne DE, Suarez DL, Sims LD.** 2013. Influenza. *In*: Diseases of poultry (Swayne DE, Glisson JR, McDougald LR, Nolan LK, Suarez DL, Nair V, eds), 13th edn. Wiley, Ames, pp 191–218

20. **Capua I, Marangon S.** 2000. The avian Influenza epidemic in Italy, 1999–2000: a review. Avian Pathol **29**:289–294
21. **Kuiken T, van den Brand J, van Riel D, Pantin-Jackwood M, Swayne DE.** 2010. Comparative pathology of select agent Influenza A virus infections. Vet Pathol **47**:893-914.
22. **Cooley AJ, Van Campen H, Philpott MS, Easterday BC, Hinshaw VS.** 1989. Pathological lesions in the lungs of ducks infected with Influenza A viruses. Vet Pathol **26**:1-5.
23. **Alexander DJ, Capua I, Koch G.** 2008. Highly pathogenic avian Influenza outbreaks in Europe, Asia, and Africa since 1959, excluding the Asian H5N1 virus outbreaks. *In*: Swayne DE (ed) avian Influenza, 1st edn. Blackwell Publishing, Ames, pp 217–237
24. **Pantin-Jackwood MJ, Swayne DE.** 2007. Pathobiology of Asian highly pathogenic avian Influenza H5N1 virus infections in ducks. Avian Dis **51**:250-9.
25. **Perkins LE, Swayne DE.** 2002. Pathogenicity of a Hong Kong-origin H5N1 highly pathogenic avian Influenza virus for emus, geese, ducks, and pigeons. Avian Dis **46**:53-63.
26. **Franca M, Stallknecht DE, Poulson R, Brown J, Howerth EW.** 2012. The pathogenesis of low pathogenic avian Influenza in mallards. Avian Dis **56**:976-80.
27. **Kida H, Yanagawa R, Matsuoka Y.** 1980. Duck Influenza lacking evidence of disease signs and immune response. Infect Immun **30**:547-53.
28. **Daoust PY, Kibenge FS, Fouchier RA, van de Bildt MW, van Riel D, Kuiken T.** 2011. Replication of low pathogenic avian Influenza virus in naturally infected Mallard ducks (Anas platyrhynchos) causes no morphologic lesions. J Wildl Dis **47**:401-9.
29. **Munster VJ, Veen J, Olsen B, Vogel R, Osterhaus AD, Fouchier RA.** 2006. Towards improved Influenza A virus surveillance in migrating birds. Vaccine **24**:6729-33.
30. **Perez, D. R.** (Ed.). 2017. Reverse Genetics of RNA Viruses. Methods in Molecular Biology. doi:10.1007/978-1-4939-6964-7
31. **Poomputsa K, Kittel C, Egorov A, Ernst W, Grabherr R.** 2003. Generation of recombinant Influenza virus using baculovirus delivery vector. J Virol Methods **110**:111-4.
32. **Enami M, Enami K.** 2000. Characterization of Influenza virus NS1 protein by using a novel helper-virus-free reverse genetic system. J Virol **74**:5556-61.
33. **Engelhardt, O. G.** 2013, Many ways to make an Influenza virus – review of Influenza virus reverse genetics methods. Influenza and Other Respiratory Viruses, **7**: 249-256.
34. **Neumann G, Watanabe T, Ito H, Watanabe S, Goto H, Gao P, Hughes M, Perez DR, Donis R, Hoffmann E, Hobom G, Kawaoka Y.** 1999. Generation of Influenza A viruses entirely from cloned cDNAs. Proc Natl Acad Sci U S A **96**:9345-50.
35. **Hoffmann E, Webster RG.** 2000. Unidirectional RNA polymerase I-polymerase II transcription system for the generation of Influenza A virus from eight plasmids. J Gen Virol **81**:2843-7.
36. **Hoffmann E, Mahmood K, Yang CF, Webster RG, Greenberg HB, Kemble G.** 2002. Rescue of Influenza B virus from eight plasmids. Proc Natl Acad Sci U S A 99:11411-6.
37. Pachler K, Mayr J, Vlasak R. 2010. A seven plasmid-based system for the rescue of Influenza C virus. J Mol Genet Med **4**:239-46.
38. **Zhang X, Kong W, Ashraf S, Curtiss R, 3rd.** 2009. A one-plasmid system to generate Influenza virus in cultured chicken cells for potential use in Influenza vaccine. J Virol **83**:9296-303.
39. **Massin P, Rodrigues P, Marasescu M, van der Werf S, Naffakh N.** 2005. Cloning of the chicken RNA polymerase I promoter and use for reverse genetics of Influenza A viruses in avian cells. J Virol **79**:13811-6.
40. **Suphaphiphat P, Keiner B, Trusheim H, Crotta S, Tuccino AB, Zhang P, Dormitzer PR, Mason PW, Franti M.** 2010. Human RNA polymerase I-driven reverse genetics for Influenza a virus in canine cells. J Virol **84**:3721-5.
41. **Tumpey TM, Basler CF, Aguilar PV, Zeng H, Solorzano A, Swayne DE, Cox NJ, Katz JM, Taubenberger JK, Palese P, Garcia-Sastre A.** 2005. Characterization of the reconstructed 1918 Spanish Influenza pandemic virus. Science **310**:77-80.

42. **Mueller S, Coleman JR, Papamichail D, Ward CB, Nimnual A, Futcher B, Skiena S, Wimmer E.** 2010. Live attenuated Influenza virus vaccines by computer-aided rational design. Nat Biotechnol **28**:723-6.
43. **Brauer R, Chen P.** 2015. Influenza virus propagation in embryonated chicken eggs. J Vis Exp doi:10.3791/52421.
44. **Madin SH, Darby NB, Jr.** 1958. Established kidney cell lines of normal adult bovine and ovine origin. Proc Soc Exp Biol Med **98**:574-6.
45. **Gaush CR, Smith TF.** 1968. Replication and plaque assay of Influenza virus in an established line of canine kidney cells. Appl Microbiol **16**:588-94.
46. **Goldstein MA, Tauraso NM, Orr HC.** 1970. Evaluation of three cell culture systems as substrates for Influenza virus assay. Appl Microbiol **19**:580-2.
47. **Meguro H, Bryant JD, Torrence AE, Wright PF.** 1979. Canine kidney cell line for isolation of respiratory viruses. J Clin Microbiol **9**:175-9.
48. **Matlin KS, Reggio H, Helenius A, Simons K.** 1981. Infectious entry pathway of Influenza virus in a canine kidney cell line. J Cell Biol **91**:601-13.
49. **Chen BJ, Leser GP, Jackson D, Lamb RA.** 2008. The Influenza virus M2 protein cytoplasmic tail interacts with the M1 protein and influences virus assembly at the site of virus budding. J Virol **82**:10059-70.
50. **Vanderlinden E, Goktas F, Cesur Z, Froeyen M, Reed ML, Russell CJ, Cesur N, Naesens L.** 2010. Novel inhibitors of Influenza virus fusion: structure-activity relationship and interaction with the viral hemagglutinin. J Virol **84**:4277-88.
51. **Roth MG, Fitzpatrick JP, Compans RW.** 1979. Polarity of Influenza and vesicular stomatitis virus maturation in MDCK cells: lack of a requirement for glycosylation of viral glycoproteins. Proc Natl Acad Sci U S A **76**:6430-4.
52. **Wandinger-Ness A, Bennett MK, Antony C, Simons K.** 1990. Distinct transport vesicles mediate the delivery of plasma membrane proteins to the apical and basolateral domains of MDCK cells. J Cell Biol **111**:987-1000.
53. **Lin SC, Kappes MA, Chen MC, Lin CC, Wang TT.** 2017. Distinct susceptibility and applicability of MDCK derivatives for Influenza virus research. PLoS One **12**:e0172299.
54. **Oh DY, Barr IG, Mosse JA, Laurie KL.** 2008. MDCK-SIAT1 cells show improved isolation rates for recent human Influenza viruses compared to conventional MDCK cells. J Clin Microbiol **46**:2189-94.
55. **Doroshenko A, Halperin SA.** 2009. Trivalent MDCK cell culture-derived Influenza vaccine Optaflu (Novartis Vaccines). Expert Rev Vaccines **8**:679-88.
56. **Govorkova EA, Murti G, Meignier B, de Taisne C, Webster RG.** 1996. African green monkey kidney (Vero) cells provide an alternative host cell system for Influenza A and B viruses. j virol **70**:5519-24.
57. **Youil R, Su Q, Toner TJ, Szymkowiak C, Kwan WS, Rubin B, Petrukhin L, Kiseleva I, Shaw AR, DiStefano D.** 2004. Comparative study of Influenza virus replication in Vero and MDCK cell lines. J Virol Methods **120**:23-31.
58. **Yao Y, Mingay LJ, McCauley JW, Barclay WS.** 2001. Sequences in Influenza A virus PB2 protein that determine productive infection for an avian Influenza virus in mouse and human cell lines. J Virol **75**:5410-5.
59. **Barrett PN, Berezuk G, Fritsch S, Aichinger G, Hart MK, El-Amin W, Kistner O, Ehrlich HJ.** 2011. Efficacy, safety, and immunogenicity of a Vero-cell-culture-derived trivalent Influenza vaccine: a multicentre, double-blind, randomised, placebo-controlled trial. Lancet **377**:751-9.
60. **Govorkova EA, Matrosovich MN, Tuzikov AB, Bovin NV, Gerdil C, Fanget B, Webster RG.** 1999. Selection of receptor-binding variants of human Influenza A and B viruses in baby hamster kidney cells. Virology **262**:31-8.
61. **Huang YT, Turchek BM.** 2000. Mink lung cells and mixed mink lung and A549 cells for rapid detection of Influenza virus and other respiratory viruses. J Clin Microbiol **38**:422-3.
62. **Sreenivasan CC, Thomas M, Antony L, Wormstadt T, Hildreth MB, Wang D, Hause B, Francis DH, Li F, Kaushik RS.** 2019. Development and characterization of swine

primary respiratory epithelial cells and their susceptibility to infection by four Influenza virus types. Virology **528**:152-163.
63. **Katz JM, Webster RG.** 1992. Amino acid sequence identity between the HA1 of Influenza A (H3N2) viruses grown in mammalian and primary chick kidney cells. J Gen Virol **73** (Pt 5):1159-65.
64. **Kaiser A, Willer T, Sid H, Petersen H, Baumgartner W, Steinberg P, Rautenschlein S.** 2016. Susceptibility of primary chicken intestinal epithelial cells for low pathogenic avian Influenza virus and velogenic viscerotropic Newcastle disease virus. Virus Res **225**:50-63.
65. **Davis RL, Choi G, Kuiken T, Quere P, Trapp S, Short KR, Richard M.** 2018. The culture of primary duck endothelial cells for the study of avian Influenza. BMC Microbiol **18**:138.
66. **Zeng H, Goldsmith CS, Kumar A, Belser JA, Sun X, Pappas C, Brock N, Bai Y, Levine M, Tumpey TM, Maines TR.** 2019. Tropism and Infectivity of a Seasonal A(H1N1) and a Highly Pathogenic Avian A(H5N1) Influenza Virus in Primary Differentiated Ferret Nasal Epithelial Cell Cultures. J Virol **93**.
67. **Ibricevic A, Pekosz A, Walter MJ, Newby C, Battaile JT, Brown EG, Holtzman MJ, Brody SL.** 2006. Influenza virus receptor specificity and cell tropism in mouse and human airway epithelial cells. J Virol **80**:7469-80.
68. **Fischer WA, 2nd, King LS, Lane AP, Pekosz A.** 2015. Restricted replication of the live attenuated Influenza A virus vaccine during infection of primary differentiated human nasal epithelial cells. Vaccine **33**:4495-504.
69. **Seo SH, Goloubeva O, Webby R, Webster RG.** 2001. Characterization of a porcine lung epithelial cell line suitable for Influenza virus studies. J Virol **75**:9517-25.
70. **Sun Z, Huber VC, McCormick K, Kaushik RS, Boon AC, Zhu L, Hause B, Webby RJ, Fang Y.** 2012. Characterization of a porcine intestinal epithelial cell line for Influenza virus production. J Gen Virol **93**:2008-16.
71. **Xie X, Gan Y, Pang M, Shao G, Zhang L, Liu B, Xu Q, Wang H, Feng Y, Yu Y, Chen R, Wu M, Zhang Z, Hua L, Xiong Q, Liu M, Feng Z.** 2018. Establishment and characterization of a telomerase-immortalized porcine bronchial epithelial cell line. J Cell Physiol **233**:9763-9776.
72. **Thomas M, Pierson M, Uprety T, Zhu L, Ran Z, Sreenivasan CC, Wang D, Hause B, Francis DH, Li F, Kaushik RS.** 2018. Comparison of Porcine Airway and Intestinal Epithelial Cell Lines for the Susceptibility and Expression of Pattern Recognition Receptors upon Influenza Virus Infection. Viruses **10**.
73. **Esnault E, Bonsergent C, Larcher T, Bed'hom B, Vautherot JF, Delaleu B, Guigand L, Soubieux D, Marc D, Quere P.** 2011. A novel chicken lung epithelial cell line: characterization and response to low pathogenicity avian Influenza virus. Virus Res **159**:32-42.
74. **Park WJ, Park BJ, Song YJ, Lee DH, Yuk SS, Lee JB, Park SY, Song CS, Lee SW, Choi IS.** 2015. Analysis of cytokine production in a newly developed canine tracheal epithelial cell line infected with H3N2 canine Influenza virus. Arch Virol **160**:1397-405.
75. **Liu G, Chen S, Hu A, Zhang L, Sun W, Chen J, Tang W, Zhang H, Liu C, Ke C, Chen X.** 2019. The Establishment and Validation of the Human U937 Cell Line as a Cellular Model to Screen Immunomodulatory Agents Regulating Cytokine Release Induced by Influenza Virus Infection. Virol Sin doi:10.1007/s12250-019-00145-w.
76. **Milian E, Kamen AA.** 2015. Current and emerging cell culture manufacturing technologies for Influenza vaccines. Biomed Res Int **2015**:504831.
77. **Pau MG, Ophorst C, Koldijk MH, Schouten G, Mehtali M, Uytdehaag F.** 2001. The human cell line PER.C6 provides a new manufacturing system for the production of Influenza vaccines. Vaccine **19**:2716-21.
78. **Le Ru A, Jacob D, Transfiguracion J, Ansorge S, Henry O, Kamen AA.** 2010. Scalable production of Influenza virus in HEK-293 cells for efficient vaccine manufacturing. Vaccine **28**:3661-71.
79. **Genzel Y, Reichl U.** 2009. Continuous cell lines as a production system for Influenza vaccines. Expert Rev Vaccines **8**:1681-92.

80. **Petiot E, Proust A, Traversier A, Durous L, Dappozze F, Gras M, Guillard C, Balloul JM, Rosa-Calatrava M.** 2018. Influenza viruses production: Evaluation of a novel avian cell line DuckCelt(R)-T17. Vaccine **36**:3101-3111.
81. **W. Garten, H.D. Klenk.** 2008. Cleavage activation of the Influenza virus hemagglutinin and its role in pathogenesis. In Avian Influenza: Monographs in Virology, vol. **27**.
82. **Russell CJ.** 2014. Acid-induced membrane fusion by the hemagglutinin protein and its role in Influenza virus biology. Curr Top Microbiol Immunol **385**:93-116.
83. **Bottcher-Friebertshauser E, Garten W, Matrosovich M, Klenk HD.** 2014. The hemagglutinin: a determinant of pathogenicity. Curr Top Microbiol Immunol **385**:3-34.
84. **Alexander DJ.** 2007. An overview of the epidemiology of avian Influenza. Vaccine **25**:5637-44.
85. **Thomas G.** 2002. Furin at the cutting edge: from protein traffic to embryogenesis and disease. Nat Rev Mol Cell Biol **3**:753-66.
86. **Hamilton BS, Whittaker GR.** 2013. Cleavage activation of human-adapted Influenza virus subtypes by kallikrein-related peptidases 5 and 12. J Biol Chem **288**:17399-407.
87. **Lu Y, Hardes K, Dahms SO, Bottcher-Friebertshauser E, Steinmetzer T, Than ME, Klenk HD, Garten W.** 2015. Peptidomimetic furin inhibitor MI-701 in combination with oseltamivir and ribavirin efficiently blocks propagation of highly pathogenic avian Influenza viruses and delays high level oseltamivir resistance in MDCK cells. Antiviral Res **120**:89-100.
88. **Kido H, Okumura Y, Yamada H, Le TQ, Yano M.** 2007. Proteases essential for human Influenza virus entry into cells and their inhibitors as potential therapeutic agents. Curr Pharm Des **13**:405-14.
89. **Bottcher E, Matrosovich T, Beyerle M, Klenk HD, Garten W, Matrosovich M.** 2006. Proteolytic activation of Influenza viruses by serine proteases TMPRSS2 and HAT from human airway epithelium. J Virol **80**:9896-8.
90. **Garten W, Braden C, Arendt A, Peitsch C, Baron J, Lu Y, Pawletko K, Hardes K, Steinmetzer T, Bottcher-Friebertshauser E.** 2015. Influenza virus activating host proteases: Identification, localization and inhibitors as potential therapeutics. Eur J Cell Biol **94**:375-83.
91. **Bottcher E, Freuer C, Steinmetzer T, Klenk HD, Garten W.** 2009. MDCK cells that express proteases TMPRSS2 and HAT provide a cell system to propagate Influenza viruses in the absence of trypsin and to study cleavage of HA and its inhibition. Vaccine **27**:6324-9.
92. **Galloway SE, Reed ML, Russell CJ, Steinhauer DA.** 2013. Influenza HA subtypes demonstrate divergent phenotypes for cleavage activation and pH of fusion: implications for host range and adaptation. PLoS Pathog **9**:e1003151.
93. **Hatesuer B, Bertram S, Mehnert N, Bahgat MM, Nelson PS, Pohlmann S, Schughart K.** 2013. Tmprss2 is essential for Influenza H1N1 virus pathogenesis in mice. PLoS Pathog **9**:e1003774.
94. **Tarnow C, Engels G, Arendt A, Schwalm F, Sediri H, Preuss A, Nelson PS, Garten W, Klenk HD, Gabriel G, Bottcher-Friebertshauser E.** 2014. TMPRSS2 is a host factor that is essential for pneumotropism and pathogenicity of H7N9 Influenza A virus in mice. J Virol **88**:4744-51.
95. **Sakai K, Ami Y, Tahara M, Kubota T, Anraku M, Abe M, Nakajima N, Sekizuka T, Shirato K, Suzaki Y, Ainai A, Nakatsu Y, Kanou K, Nakamura K, Suzuki T, Komase K, Nobusawa E, Maenaka K, Kuroda M, Hasegawa H, Kawaoka Y, Tashiro M, Takeda M.** 2014. The host protease TMPRSS2 plays a major role in in vivo replication of emerging H7N9 and seasonal Influenza viruses. J Virol **88**:5608-16.
96. **Bertram S, Glowacka I, Blazejewska P, Soilleux E, Allen P, Danisch S, Steffen I, Choi SY, Park Y, Schneider H, Schughart K, Pohlmann S.** 2010. TMPRSS2 and TMPRSS4 facilitate trypsin-independent spread of Influenza virus in Caco-2 cells. J Virol **84**:10016-25.
97. **Kuhn N, Bergmann S, Kosterke N, Lambertz RLO, Keppner A, van den Brand JMA, Pohlmann S, Weiss S, Hummler E, Hatesuer B, Schughart K.** 2016. The Proteolytic

Activation of (H3N2) Influenza A Virus Hemagglutinin Is Facilitated by Different Type II Transmembrane Serine Proteases. J Virol **90**:4298-4307.

98. **Hamilton BS, Gludish DW, Whittaker GR.** 2012. Cleavage activation of the human-adapted Influenza virus subtypes by matriptase reveals both subtype and strain specificities. J Virol **86**:10579-86.
99. **Baron J, Tarnow C, Mayoli-Nussle D, Schilling E, Meyer D, Hammami M, Schwalm F, Steinmetzer T, Guan Y, Garten W, Klenk HD, Bottcher-Friebertshauser E.** 2013. Matriptase, HAT, and TMPRSS2 activate the hemagglutinin of H9N2 Influenza A viruses. J Virol **87**:1811-20.
100. **Beaulieu A, Gravel E, Cloutier A, Marois I, Colombo E, Desilets A, Verreault C, Leduc R, Marsault E, Richter MV.** 2013. Matriptase proteolytically activates Influenza virus and promotes multicycle replication in the human airway epithelium. J Virol **87**:4237-51.
101. **Zmora P, Blazejewska P, Moldenhauer AS, Welsch K, Nehlmeier I, Wu Q, Schneider H, Pohlmann S, Bertram S.** 2014. DESC1 and MSPL activate Influenza A viruses and emerging coronaviruses for host cell entry. J Virol **88**:12087-97.
102. **Hamilton BS, Whittaker GR.** 2013. Cleavage activation of human-adapted Influenza virus subtypes by kallikrein-related peptidases 5 and 12. J Biol Chem **288**:17399-407.
103. **Magnen M, Gueugnon F, Guillon A, Baranek T, Thibault VC, Petit-Courty A, de Veer SJ, Harris J, Humbles AA, Si-Tahar M, Courty Y.** 2017. Kallikrein-Related Peptidase 5 Contributes to H3N2 Influenza Virus Infection in Human Lungs. J Virol **91**.
104. **Zmora P, Hoffmann M, Kollmus H, Moldenhauer AS, Danov O, Braun A, Winkler M, Schughart K, Pohlmann S.** 2018. TMPRSS11A activates the Influenza A virus hemagglutinin and the MERS coronavirus spike protein and is insensitive against blockade by HAI-1. J Biol Chem **293**:13863-13873.
105. **Tanikawa T, Uchida Y, Saito T.** 2017. Replication of a low-pathogenic avian Influenza virus is enhanced by chicken ubiquitin-specific protease 18. J Gen Virol **98**:2235-2247.
106. **Chaipan C, Kobasa D, Bertram S, Glowacka I, Steffen I, Tsegaye TS, Takeda M, Bugge TH, Kim S, Park Y, Marzi A, Pohlmann S.** 2009. Proteolytic activation of the 1918 Influenza virus hemagglutinin. J Virol **83**:3200-11.
107. **Peitsch C, Klenk HD, Garten W, Bottcher-Friebertshauser E.** 2014. Activation of Influenza A viruses by host proteases from swine airway epithelium. J Virol **88**:282-91.
108. **Meyer D, Sielaff F, Hammami M, Bottcher-Friebertshauser E, Garten W, Steinmetzer T.** 2013. Identification of the first synthetic inhibitors of the type II transmembrane serine protease TMPRSS2 suitable for inhibition of Influenza virus activation. Biochem J **452**:331-43.
109. **Xiong X, McCauley JW, Steinhauer DA.** 2014. Receptor binding properties of the Influenza virus hemagglutinin as a determinant of host range. Curr Top Microbiol Immunol **385**:63-91.
110. **Skehel JJ, Wiley DC.** 2000. Receptor binding and membrane fusion in virus entry: the Influenza hemagglutinin. Annu Rev Biochem **69**:531-69.
111. **Glaser L, Stevens J, Zamarin D, Wilson IA, Garcia-Sastre A, Tumpey TM, Basler CF, Taubenberger JK, Palese P.** 2005. A single amino acid substitution in 1918 Influenza virus hemagglutinin changes receptor binding specificity. J Virol **79**:11533-6.
112. **Stevens J, Blixt O, Glaser L, Taubenberger JK, Palese P, Paulson JC, Wilson IA.** 2006. Glycan microarray analysis of the hemagglutinins from modern and pandemic Influenza viruses reveals different receptor specificities. J Mol Biol **355**:1143-55.
113. **Shinya K, Ebina M, Yamada S, Ono M, Kasai N, Kawaoka Y.** 2006. Avian flu: Influenza virus receptors in the human airway. Nature **440**:435-6.
114. **Nicholls JM, Bourne AJ, Chen H, Guan Y, Peiris JS.** 2007. Sialic acid receptor detection in the human respiratory tract: evidence for widespread distribution of potential binding sites for human and avian Influenza viruses. Respir Res **8**:73.
115. **Nelli RK, Kuchipudi SV, White GA, Perez BB, Dunham SP, Chang KC.** 2010. Comparative distribution of human and avian type sialic acid Influenza receptors in the pig. BMC Vet Res **6**:4.

116. **Trebbien R, Larsen LE, Viuff BM.** 2011. Distribution of sialic acid receptors and Influenza A virus of avian and swine origin in experimentally infected pigs. Virol J **8**:434.
117. **Bateman AC, Karamanska R, Busch MG, Dell A, Olsen CW, Haslam SM.** 2010. Glycan analysis and Influenza A virus infection of primary swine respiratory epithelial cells: the importance of NeuAc{alpha}2-6 glycans. J Biol Chem **285**:34016-26.
118. **Chan RW, Karamanska R, Van Poucke S, Van Reeth K, Chan IW, Chan MC, Dell A, Peiris JS, Haslam SM, Guan Y, Nicholls JM.** 2013. Infection of swine ex vivo tissues with avian viruses including H7N9 and correlation with glycomic analysis. Influenza Other Respir Viruses **7**:1269-82.
119. **Kuchipudi SV, Nelli R, White GA, Bain M, Chang KC, Dunham S.** 2009. Differences in Influenza virus receptors in chickens and ducks: Implications for interspecies transmission. J Mol Genet Med **3**:143-51.
120. **Costa T, Chaves AJ, Valle R, Darji A, van Riel D, Kuiken T, Majo N, Ramis A.** 2012. Distribution patterns of Influenza virus receptors and viral attachment patterns in the respiratory and intestinal tracts of seven avian species. Vet Res **43**:28.
121. **Baumann J, Kouassi NM, Foni E, Klenk HD, Matrosovich M.** 2016. H1N1 Swine Influenza Viruses Differ from Avian Precursors by a Higher pH Optimum of Membrane Fusion. J Virol **90**:1569-77.
122. **Russier M, Yang G, Rehg JE, Wong SS, Mostafa HH, Fabrizio TP, Barman S, Krauss S, Webster RG, Webby RJ, Russell CJ.** 2016. Molecular requirements for a pandemic Influenza virus: An acid-stable hemagglutinin protein. Proc Natl Acad Sci U S A **113**:1636-41.
123. **Lancaster, J. E.** 1976. A History of Newcastle Disease with Comments on its Economic Effects. World's Poultry Science Journal, **32**(02), 167–175.
124. **Mayo MA.** 2002. A summary of taxonomic changes recently approved by ICTV. Arch Virol **147**:1655-63.
125. **Lamb, R. A., Parks, G. D.** 2007. Paramyxoviridae: the viruses and their replication. *In* B. N. Fields, D. N. Knipe, & P. M. Howley (Eds.), Fields virology: Fifth Edition (5 ed., pp. 1449-1496).
126. **Steward M, Vipond IB, Millar NS, Emmerson PT.** 1993. RNA editing in Newcastle disease virus. J Gen Virol **74** (Pt 12):2539-47.
127. Hanson RP, Brandly CA. 1955. Identification of vaccine strains of Newcastle disease virus. Science 122:156-7.
128. **World Organisation for Animal Health (OIE).** 2018. Chapter 3.3.14. Newcastle disease. In Terrestrial Manual 964-983.
129. **Choi KS, Lee EK, Jeon WJ, Kwon JH.** 2010. Antigenic and immunogenic investigation of the virulence motif of the Newcastle disease virus fusion protein. J Vet Sci **11**:205-11.
130. **Nagai Y.** 1993. Protease-dependent virus tropism and pathogenicity. Trends Microbiol **1**:81-7.
131. **Panda A, Huang Z, Elankumaran S, Rockemann DD, Samal SK.** 2004. Role of fusion protein cleavage site in the virulence of Newcastle disease virus. Microb Pathog **36**:1-10.
132. **Dortmans JC, Rottier PJ, Koch G, Peeters BP.** 2010. The viral replication complex is associated with the virulence of Newcastle disease virus. J Virol **84**:10113-20.
133. **Dortmans JC, Koch G, Rottier PJ, Peeters BP.** 2011. Virulence of Newcastle disease virus: what is known so far? Vet Res **42**:122.
134. **Girling, S. J. and Girling, S. J.** 2013. Basic Avian Anatomy and Physiology, p 131-19, Veterinary Nursing of Exotic Pets S. J. Girling (Ed.). doi:10.1002/9781118782941.ch9.
135. **Turk DE.** 1982. The anatomy of the avian digestive tract as related to feed utilization. Poult Sci **61**:1225-44.
136. **Klasing KC.** 1999. Avian gastrointestinal anatomy and physiology. Seminars in Avian and Exotic Pet Medicine **8**:42-50.
137. **Kierończyk B, Rawski M, Długosz J, Świątkiewicz S, Józefiak D.** 2016. Avian Crop Function – A Review. **16**:653.
138. **Langlois I.** 2003. The anatomy, physiology, and diseases of the avian proventriculus and ventriculus. Vet Clin North Am Exot Anim Pract **6**:85-111.

139. **Svihus B.** 2011. The gizzard: Function, influence of diet structure and effects on nutrient availability. World's Poultry Science Journal. **67**. 207 - 224.
140. **Kato T, Owen R.** 2005. Structure and function of intestinal mucosal epithelium. **10**.1016/B978-012491543-5/50012-7.
141. **Koutsos EA, Arias VJ.** 2006. Intestinal Ecology: Interactions Among the Gastrointestinal Tract, Nutrition, and the Microflora. The Journal of Applied Poultry Research **15**:161-173.
142. **Svihus B., Choct M., Classen H.** 2013. Function and nutritional roles of the avian caeca: A review. World's Poultry Science Journal, **69**(2), 249-264.
143. **Pubols MH.** 1991. Ratio of digestive enzymes in the chick pancreas. Poult Sci **70**:337-42.
144. **Pilny AA.** 2008. The avian pancreas in health and disease. Vet Clin North Am Exot Anim Pract **11**:25-34, v-vi.
145. **Zaefarian F, Abdollahi MR, Cowieson A, Ravindran V.** 2019. Avian Liver: The Forgotten Organ. Animals (Basel) **9**.
146. **Wagner R, Gabriel G, Schlesner M, Alex N, Herwig A, Werner O, Klenk HD.** 2013. Protease activation mutants elicit protective immunity against highly pathogenic avian Influenza viruses of subtype H7 in chickens and mice. Emerg Microbes Infect **2**:e7.
147. **Klenk HD, Rott R, Orlich M, Blodorn J.** 1975. Activation of Influenza A viruses by trypsin treatment. Virology **68**:426-39.
148. **Lazarowitz SG, Choppin PW.** 1975. Enhancement of the infectivity of Influenza A and B viruses by proteolytic cleavage of the hemagglutinin polypeptide. Virology **68**:440-54.
149. **Scholtissek C.** 1985. Stability of infectious Influenza A viruses at low pH and at elevated temperature. Vaccine **3**:215-8.
150. **Ottis K, Bachmann PA.** 1980. Occurrence of Hsw 1 N 1 subtype Influenza A viruses in wild ducks in Europe. Arch Virol **63**:185-90.
151. **Schafer W, Stroh A, Berghofer S, Seiler J, Vey M, Kruse ML, Kern HF, Klenk HD, Garten W.** 1995. Two independent targeting signals in the cytoplasmic domain determine trans-Golgi network localization and endosomal trafficking of the proprotein convertase furin. Embo j **14**:2424-35.
152. **Witkowski PT, Perley CC, Brocato RL, Hooper JW, Jurgensen C, Schulzke JD, Kruger DH, Bucker R.** 2017. Gastrointestinal Tract As Entry Route for Hantavirus Infection. Front Microbiol **8**:1721.
153. **Zhou J, Li C, Zhao G, Chu H, Wang D, Yan HH, Poon VK, Wen L, Wong BH, Zhao X, Chiu MC, Yang D, Wang Y, Au-Yeung RKH, Chan IH, Sun S, Chan JF, To KK, Memish ZA, Corman VM, Drosten C, Hung IF, Zhou Y, Leung SY, Yuen KY.** 2017. Human intestinal tract serves as an alternative infection route for Middle East respiratory syndrome coronavirus. Sci Adv **3**:eaao4966.
154. **Weiss C, Clark HF.** 1985. Rapid inactivation of rotaviruses by exposure to acid buffer or acidic gastric juice. J Gen Virol **66** (Pt 12):2725-30.
155. **Beasley DE, Koltz AM, Lambert JE, Fierer N, Dunn RR.** 2015. The Evolution of Stomach Acidity and Its Relevance to the Human Microbiome. PLoS One **10**:e0134116.
156. **Post J, Burt DW, Cornelissen JB, Broks V, van Zoelen D, Peeters B, Rebel JM.** 2012. Systemic virus distribution and host responses in brain and intestine of chickens infected with low pathogenic or high pathogenic avian Influenza virus. Virol J **9**:61.
157. **Meulemans G, Gonze M, Carlier MC, Petit P, Burny A, Long L.** 1986. Protective effects of HN and F glycoprotein-specific monoclonal antibodies on experimental Newcastle disease. Avian Pathol **15**:761-8.
158. **Tate MD, Job ER, Deng YM, Gunalan V, Maurer-Stroh S, Reading PC.** 2014. Playing hide and seek: how glycosylation of the Influenza virus hemagglutinin can modulate the immune response to infection. Viruses **6**:1294-316.
159. **Cruz E, Cain J, Crossett B, Kayser V.** 2018. Site-specific glycosylation profile of Influenza A (H1N1) hemagglutinin through tandem mass spectrometry. Hum Vaccin Immunother **14**:508-517.
160. **Ito T, Suzuki Y, Suzuki T, Takada A, Horimoto T, Wells K, Kida H, Otsuki K, Kiso M, Ishida H, Kawaoka Y.** 2000. Recognition of N-glycolylneuraminic acid linked to galactose

by the alpha2,3 linkage is associated with intestinal replication of Influenza A virus in ducks. J Virol **74**:9300-5.

Publications

Han X, Bertzbach LD, Veit M. 2019. Mimicking the passage of avian Influenza viruses through the gastrointestinal tract of chickens. **Veterinary Microbiology.**

Han X, Veit M. 2019. Characterization of novel chicken intestinal epithelial cell lines susceptible to Influenza Virus and Newcastle Disease Virus study. (in preparation)

Acknowledgements

In the end of my PhD study, I would express my appreciation to many people who give me help and support in these years.

Firstly, I am deeply grateful to my supervisor, Dr. Michael Veit. He always gives precious suggestions and guidance when I get stuck in my study, and always encourages me when I am upset about myself. I have not only obtained knowledge, but also rigorous academic attitude from him. I would also like to express my thanks to my second supervisor Dr. Benedikt Kaufer and my mentor Dr. Kasten Tedin for their valuable suggestions and supports.

I am particularly grateful to all the members in Dr. Veit's lab for their accompany and help. Thanks to Dr. Chris Höfer, Dr. Ludwig Krabben, Dr. Susanne Kaufer, Dr. Minze Zhang, PhD students Bodan Hu, Mohamed Rasheed Gadalla, Atika Hadiati. Thanks to technician Mrs. Elke Dyrks and Mrs. Angelika Thomele for their assistant in the lab and in daily life.

I would also appreciate the help from all the members of Institute of Virology. Special thanks to Dr. Luca Danilo Bertzbach for his help with chicken sample collection. Thanks to Prof. Klaus Osterrieder, Dr. Walid Azab, Dr. Darren J. Wight, Dr. Dusan Kunec for their suggestions in each lab meeting. Thanks to Pavulraj, Ahmed, Nicole, Anirban, Na, Oleksandr and Yu. Thanks to technicians Annett, Ann and Michaela, secretary Kia.

Many thanks to my dearest parents, family and friends, I couldn't be so strong without their constant love and support.

Finally, I am grateful to the China Scholarship Coucil (CSC) for the financial support.

Selbständigkeitserklärung

Hiermit bestätige ich, dass ich die vorliegende Arbeit selbständig angefertigt habe. Ich versichere, dass ich ausschließlich die angegebenen Quellen und Hilfen Anspruch genommen habe.

Berlin, am 17.01.2020

Xuejiao HAN